Foundation Reuse:
Length, Condition, and Capacity of Existing Driven Piles

Prepared by:
  Andrew Z. Boeckmann
  Brent L. Rosenblad
  John J. Bowders
  University of Missouri-Columbia, Department of Civil and Environmental Engineering

TECHNICAL REPORT DOCUMENTATION PAGE

1. Report No.: cmr 18-008	2. Government Accession No.:	3. Recipient's Catalog No.:
4. Title and Subtitle: Foundation Reuse: Length, Condition, and Capacity of Existing Driven Piles		5. Report Date: May 2018 Published: May 2018
		6. Performing Organization Code:
7. Author(s): Andrew Z. Boeckmann https://orcid.org/0000-0003-1243-4677 Brent L. Rosenblad https://orcid.org/0000-0002-0447-4882 John J. Bowders https://orcid.org/0000-0001-6383-3980		8. Performing Organization Report No.:
9. Performing Organization Name and Address: University of Missouri-Columbia Department of Civil & Environmental Engineering E 2509 Lafferre Hall, Columbia, MO 65211		10. Work Unit No.:
		11. Contract or Grant No.: MoDOT project# TR201714
12. Sponsoring Agency Name and Address: Missouri Department of Transportation (SPR) Construction and Materials Division P.O. Box 270, Jefferson City, MO 65102		13. Type of Report and Period Covered: Final Report (January 2017-February 2018)
		14. Sponsoring Agency Code:

16. Abstract:

Reusing existing bridge foundations is an appealing design alternative for many bridge projects, but methods for investigating and analyzing existing foundations vary widely. Researchers from the University of Missouri performed research to evaluate various methods for predicting the installed length, assessing the condition, and predicting the load capacity of existing foundations. The methods were evaluated via application to two MoDOT bridges, both built in the 1960s and replaced in 2017. One bridge was founded on driven closed-end steel pipe piles backfilled with concrete (CIP piles), and the other was founded on octagonal precast concrete piles. The foundations were not actual candidates for reuse, but were selected for study because of the age and type of piles. To perform the evaluations, researchers gathered and made predictions from historical records, performed various geophysical test methods to predict pile length and potentially identify deterioration, performed static load testing, performed high-strain dynamic analyses of pile restrikes, and exhumed the piles to assess true pile length and condition.

The research found that historical pile driving records could be used to predict pile length within 3 percent of the exhumed length whereas values from as-built plans were as much as 30 percent less than the exhumed length. Results from parallel seismic testing produced estimates of pile length that were within 8 percent of the exhumed length. Parallel seismic results were more accurate when the sensor was located within 5 ft of the pile. MoDOT's seismic cone penetration test (SCPT) rig was effective for parallel seismic tests. Sonic Echo / Impulse Response test methods performed after bridge demolition were effective in predicting pile lengths for the CIP piles, but application to the precast piles underpredicted lengths by as much as 20 percent, most likely because of the taper in the precast piles. SE/IR tests performed prior to bridge demolition were mostly inconclusive, mostly because of complex vibrations between the pile and connected superstructure. Observations of exhumed piles for both CIP and precast piles revealed no significant deterioration. CIP piles had visible surface corrosion, but caliper measurements of wall thickness at sections cut through the most corroded portions were not significantly different from measurements through portions without visible corrosion. Estimates of axial load capacity of the existing foundations varied widely. Values listed on historical documents were the least, and quite conservative compared to values from static load testing. The CIP test pile was loaded to four times the historical design capacity, and the precast test pile was loaded to seven times the historical design capacity. Maximum load test values can be considered lower bound values since the tests terminated upon failure of the capping beam for the existing bridge, which was used as the reaction. Dynamic analysis of restrike data yielded estimates of axial capacity similar to the maximum loads applied during static load testing. The dynamic values are also lower bound values because the restrike hammer had insufficient energy to transfer significant load to the pile tips.

17. Key Words: Bearing capacity; Bridge foundations; Condition surveys; Geotechnical engineering; Highway bridges; Load tests; Traffic loads. Foundation reuse; Pile length; Condition assessment; Geophysical methods; Deep foundations.		18. Distribution Statement: No restrictions. This document is available through the National Technical Information Service, Springfield, VA 22161.	
19. Security Classification (of this report): Unclassified.	20. Security Classification (of this page): Unclassified.	21. No of Pages: 70	22. Price:

Form DOT F 1700.7 (06/98).

Foundation Reuse: Length, Condition, and Capacity of Existing Driven Piles

prepared for

Missouri Department of Transportation

by

Andrew Z. Boeckmann, Brent L. Rosenblad, and John J. Bowders

University of Missouri
Department of Civil and Environmental Engineering

May 2018

Acknowledgements

Table of Contents

Table of Figures

1. Introduction

1.1   Motivation and Challenges

Most U.S. transportation agencies face a significant backlog of bridges in need of replacement, with additional bridges quickly approaching the end of their useful life. Reusing the existing foundations for the replacement bridge is an appealing approach, primarily because it reduces construction costs and shortens project schedules and therefore reduces mobility impacts. Foundation reuse is also beneficial in cases where right-of-way, environmental, or historical preservation constraints make construction of new foundations difficult or impossible. In addition, foundation reuse is consistent with the emphasis some agencies have placed on sustainability.

Foundation reuse presents several significant engineering challenges. FHWA's Foundation Characterization Program hosted a workshop regarding foundation reuse in 2013, and the participants identified four major challenges:

1. Condition assessment: How much has the foundation deteriorated?
2. Load capacity: What is the ultimate resistance of the existing foundation?
3. Remaining service life: How many more years can the foundation be expected to satisfy serviceability requirements?
4. Design codes: How should the existing foundation be considered in the context of design codes?

NCHRP Synthesis Report 505 *Current Practices and Guidelines for the Reuse of Bridge Foundations* (Boeckmann and Loehr, 2017) identified two additional challenges related to legal risks. First, the allocation of risk among transportation agencies, consulting engineers, and construction contractors is unclear – even more so than for construction of new foundations. Second, the unclear allocation of risk creates an uncertain standard of care for foundation reuse design engineers.

The uncertain standard of care is reflected in a lack of policy or procedural guidance related to foundation reuse. NCHRP Synthesis Report 505 included a survey of all U.S. transportation agencies, with 45 responding. As shown in Figure 1, nearly every agency indicated it has reused foundations, but only five have policies or guidance related to reuse. None of the available guidance documents is comprehensive; most are narrowly tailored to specific reuse applications, techniques for investigation of specific types of existing foundations, or specific capacity calculation methods.
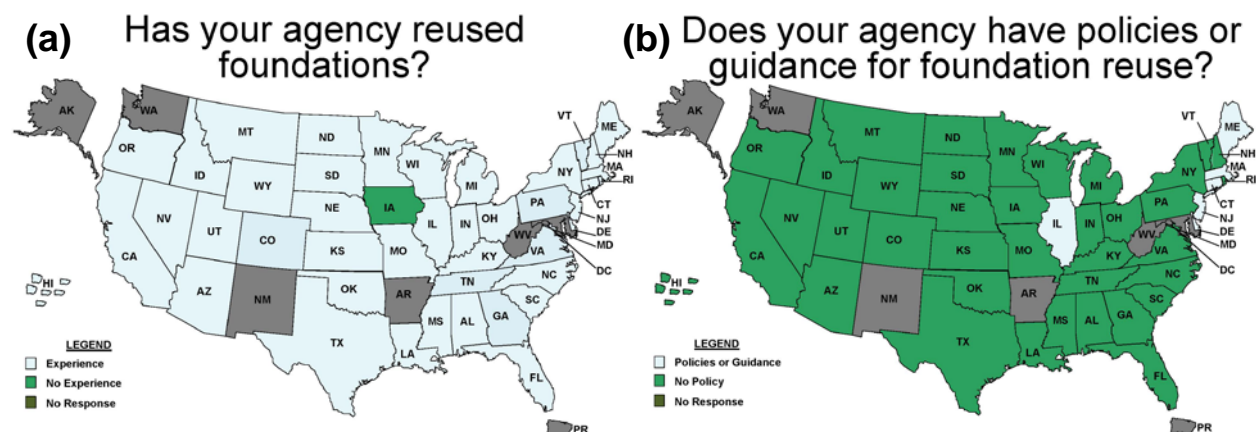
Figure 1: Results of survey for NCHRP Synthesis Report 505 regarding (a) prevalence of foundation reuse and (b) lack of foundation reuse guidance. Reused with permission.

1.2   Project Objectives and Overview

The goal of this research project is to evaluate various practices for the investigation and analysis of existing foundations under consideration for reuse. Specifically, the research will evaluate different methods for (1) predicting the installed length of existing foundations, (2) assessing the condition of existing foundations, and (3) predicting the load capacity of existing foundations. Results of the research will provide information on the potential advantages and limitations of each method for addressing the challenges outlined in the previous section. Eventually, information from the results could be used to aid the development of a guidance manual for foundation reuse.

The research for this project was performed on driven piles supporting two MoDOT bridges on low-volume roads in southeastern Missouri. The research involved

- Gathering MoDOT records regarding the project sites, existing bridges, and existing foundations
- Using the historical records to predict pile length and pile capacity using static methods
- Performing various geophysical methods to predict pile length and potentially identify any significant deterioration
- Performing a static foundation load test on one pile at each bridge
- Repeating the geophysical tests after demolition of the bridges
- Restriking the existing piles and performing high-strain dynamic analyses to predict load capacity
- Exhuming the piles and subsequently assessing true pile length and performing condition assessment, which included cross-sectional cuts at various points along the length of the piles

Both study bridges were replaced during the summer of 2017. Both bridges were constructed in the 1960s and founded on driven piles, with one bridge on closed-end steel pipe piles backfilled with concrete (cast-in-place, or CIP piles) and the other on octagonal precast concrete piles. Neither foundation was ever considered for reuse during design of the replacement bridges. The bridges were chosen for research study because the age of the driven piles provides a useful opportunity to evaluate deterioration, the pile lengths are reasonable for exhumation, and the open access and low traffic volume at both sites make performing field test methods relatively practical.

Chapter 2 of this report provides background information regarding the length, condition, and load capacity of existing deep foundations. Methods evaluated for this research project are presented in Chapter 3, with results of the research presented and discussed in Chapter 4. Conclusions are presented in Chapter 5.

2. Background

This chapter presents an introduction to important technical concepts related to foundation reuse. The topics presented below are consistent with the three primary focus areas for the project research: length, condition, and load capacity of existing deep foundations. Additional information regarding the topics below is presented in NCHRP Synthesis 505 (Boeckmann and Loehr, 2017), and in the European manual *Reuse of Foundations for Urban Sites: A Best Practice Handbook* (Butcher et al., 2006; aka the RuFUS manual).

2.1   Length of Existing Deep Foundations

Determining the length of existing deep foundations is critical for evaluations of foundation reuse. Without knowledge of deep foundation length, it is virtually impossible to evaluate axial load capacity, lateral load capacity, and scour susceptibility. Two groups of methods for determining the length of existing foundations are presented in this section. The first involves use of agency records from design, construction, and inspection. The second involves geophysical methods, which include pile integrity test methods, surface methods, and borehole methods.

2.1.1   Agency Records

Agency records include all historical documentation regarding design, construction, and inspection. Construction plans typically include foundation length information. However, the planned length of foundations often changes throughout the design process, and typically installed foundation length is different from planned foundation length, often greatly. Therefore, the best records of foundation length are typically from the most recent documentation, with as-built plans or foundation installation logs preferred over final construction plans. Foundation installation records (e.g. pile driving logs, drilled shaft installation records) are advantageous because they typically include additional information that can be used to predict load capacity (e.g. pile driving penetration resistance, drilled shaft installation geology). Agency design and construction specifications from the date of foundation installation may also provide valuable information regarding typical foundation geometry or construction practices, especially agency provisions regarding minimum foundation embedment depths.

The survey for NCHRP Synthesis 505 revealed nearly every agency that reuses bridge foundations relies on historical records, with 48 of 49 respondents acknowledging use of historical records as a method employed by their agency. However, the availability and quality of information from the agency records was found to vary, as shown in Figure 2. About half of respondents indicated records were "usually available," with just less than one-third of respondents describing the records as "always available." Nearly two-thirds of respondents indicated the historical records include "most information regarding foundation type, plan location, and dimensions." Most of the remaining respondents indicated a better scenario: the historical records "always indicate foundation type, plan location, and dimensions." However, the results do not indicate whether the foundation information in the historical records is from final plans or as-built documentation.

(a)

- Always available — 14, 29%
- Usually available — 24, 49%
- Sometimes available — 11, 22%
- Never available (0 responses)

(b)

- Historic records always indicate foundation type, plan location, and dimensions. — 15, 31%
- Historic records include most information regarding foundation type, plan location, and dimensions. — 31, 63%
- Information regarding foundation type, plan location, or dimensions is frequently missing from or conflicting in historic records. — 3, 6%
- Information regarding foundation type, plan location, or dimensions is always or almost always missing from or conflicting in historic records. (0 responses)

Figure 2: Results from survey of NCHRP Synthesis 505 regarding (a) the availability of and (b) the quality of information from historical records. Reused with permission.

2.1.2   Geophysical Methods

There are several geophysical methods that can be applied to the problem of identifying the unknown length of existing foundations. These methods can be broadly organized into pile integrity test methods, borehole methods, and surface methods. Pile integrity test methods involve impacting the top of the pile to excite compression waves in the pile with the intent of detecting the arrival of a tip reflection using a sensor mounted at the top of the foundation. Analyses performed using data recorded in the time domain are called Sonic Echo (SE) while analysis performed in the frequency domain are termed Impulse-Response (IR). The general equipment setup used for SE/IR testing is illustrated in Figure 3a. Similar approaches can be applied using bending waves or with multiple wave modes recorded with three-component receivers, termed ultraseismic.

The second general approach involves the use of a borehole installed near the pile to collect data from waves radiating outward from the pile. The method involves placing a sensor (either a geophone or hydrophone if using a water filled borehole) at a known depth in the borehole and striking vertically on the surface above the pile of interest. Compression waves propagate down the pile at the compression wave velocity of the pile and radiate out into the soil at an angle governed by Snell's law, as illustrated in Figure 3b. Assuming uniform soil conditions, a plot of wave arrivals obtained at locations above the tip of the pile should have a slope that is equal to the wave velocity in the pile. When the sensor is positioned at depths below the tip elevation the slope will change to the velocity of the soil. The depth at which the slope changes can be used to estimate the pile tip depth. Either compression or shear waves radiating from the pile can be detected and used in the analysis. It is recommended that the borehole should be within 5 ft of the pile location and should extend at least 10 to 15 ft below the base of the borehole (Wightman et al. 2004). A similar approach called cross-borehole tomography uses two boreholes on either side the pile to generate an image of the subsurface. Surface methods such as Spectral-Analysis-of-Surface-Waves (SASW), seismic reflection and seismic refraction have been attempted to identify the depth of foundations from the change in stiffness with limited success. A recent approach using Full Waveform

Inversion (FWI) has shown some promising results. Electrical methods such as resistivity and induced polarization (IP) have also been successfully applied to unknown foundation problems.
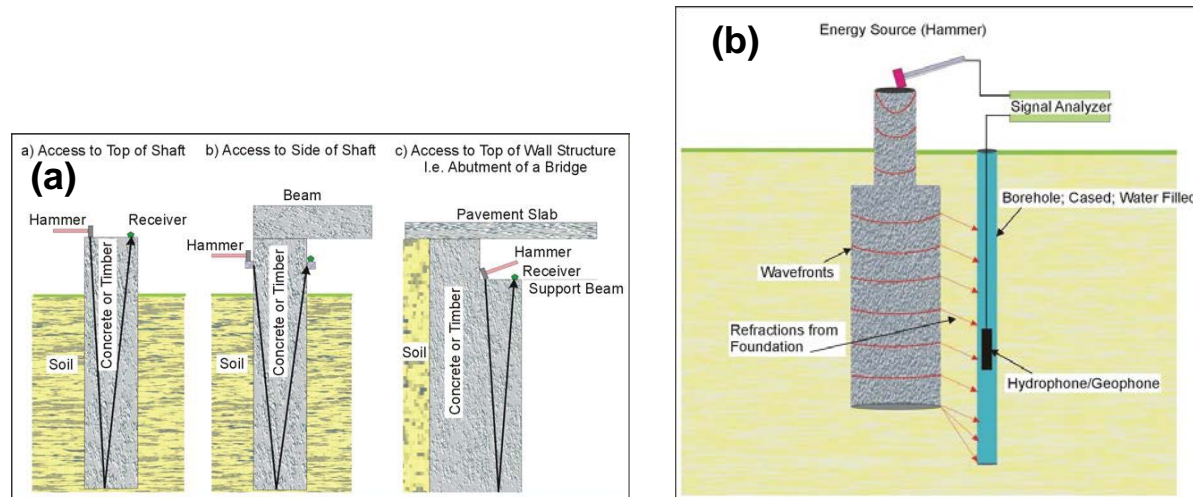
Figure 3: General testing arrangement for performing (a) SE/IR measurements with different foundation configurations and (b) Parallel Seismic measurements. Reused with permission.

2.2   Condition of Existing Deep Foundations

Uncertainty in the condition of existing foundations is likely the biggest impediment to reusing foundations. Compounding the uncertainty is the fact that evaluating the condition of existing deep foundations is typically difficult. In fact, two of the four foundation reuse challenges identified by FHWA relate to condition: the challenge of condition assessment, and the challenge of predicting remaining service life. Although investigating the condition of existing deep foundations is typically difficult, engineers have successfully used various methods to evaluate condition. Several of the methods are summarized in the sections below. The first section involves use of historical inspection records, the second involves direct observation using test pits, concrete cores, and/or steel coupons, and the last approach involves geophysical methods.

2.2.1   Inspection Records

Bridge inspection records may contain information regarding the condition of existing foundations. The National Bridge Inspection Standards (NBIS) do not explicitly require inspection of bridge foundation elements, but foundation condition information may be included with substructure inspection results. Underwater bridge inspections, in particular, tend to collect significant amounts of information regarding foundation elements above the mudline. FHWA's *Underwater Bridge Inspection* manual (Browne et al., 2010) details procedures for conducting such inspections, which FHWA classifies into three levels. Level I inspections involve visual and tactile observations without cleaning of the element to be inspected. Level II is a more detailed inspection that includes partial cleaning of the element. Level III is a "highly detailed" inspection with nondestructive testing or partially destructive testing. The manual also describes procedures for scour investigations. Roughly half of U.S. agencies will not consider foundation reuse for bridges requiring scour counter-measures (Boeckmann and Loehr, 2017).

2.2.2   Test Pits, Steel Coupons, and Concrete Coring

Direct methods to investigate the condition of existing foundations include several destructive or partially destructive techniques. Test pits involve excavating to expose the deep foundation element as shown in the example of Figure 4. Test pits are useful because they allow direct observation of significant portions of the foundation elements, and often the portions exposed (near the ground surface) are in the area of groundwater fluctuation that is most associated with corrosion. However, excavation of test pits is typically limited to relatively shallow depths, and in some cases may not be feasible (to any depth) because of

groundwater, right-of-way, traffic, or other concerns. Just more than half of the agencies responding to the NCHRP Synthesis 505 survey indicated they had used test pits to investigate the condition of existing foundations.

Figure 4: Test pit exposing timber piling. From Johnson and Chauvin (2013).

When steel H-piles are exposed by the test pits, it is typically possible to measure the thickness of the steels to supplement visual observations of any corrosion. In some cases, steel coupons may also be sampled from steel pile exposed by test pits. Tensile tests are typically performed on the coupons. One fifth of respondents to the NCHRP survey indicated their agency had performed such testing.

Concrete coring is frequently performed to visually inspect embedded concrete, and to perform laboratory tests (e.g. compressive strength, chloride content, etc.) on the core samples. For foundation reuse applications, coring can be performed on spread footings, pile caps, precast or cast-in-place concrete piles, and drilled shafts. In addition, FHWA has demonstrated the value of geophysical logging technology through core holes to provide a more comprehensive evaluation of foundation durability (Jalinoos, 2015; Jalinoos et al., 2016). Just less than half of agencies responding to the NCHRP Synthesis 505 survey indicated they had performed concrete core drilling to investigate existing foundations.

2.2.3   Geophysical Methods

Pile integrity methods described in Section 2.1.2 can also be used to detect problems with the condition of piles. Wave reflection will occur from any change in impedance, which is the product of the velocity, density and area. Therefore, changes in the cross sectional area or regions of lower stiffness or density may be detected by an additional wave reflection from within the pile. In addition, a break in the pile should be detected as an early reflected arrival. Borehole methods, such as Parallel Seismic will likely only detect large flaws in the pile that create a large disruption in the propagating energy. +Electrical methods can be used to evaluate corrosion of steel piling.

2.3   Capacity of Existing Deep Foundations

The load capacity of an existing foundation is, of course, a critical parameter in reuse decisions. Engineers have used several different methods for predicting the capacity of existing foundations, as shown in Figure 5 from the survey of NCHRP Synthesis 505. Survey respondents were asked to select any and all methods they had used, which is why the sum of the percentage values is greater than 100. Additional information on the various methods for predicting capacity of existing foundations are presented in the sections below, which organize the methods into two categories. The first category,

"desk" methods, includes capacity prediction methods that do not necessarily require collection of additional field data, although many of the desk methods yield better results when they are based on new subsurface investigation information. The second category, field load tests, includes various methods for field testing the existing foundations in order to predict capacity.
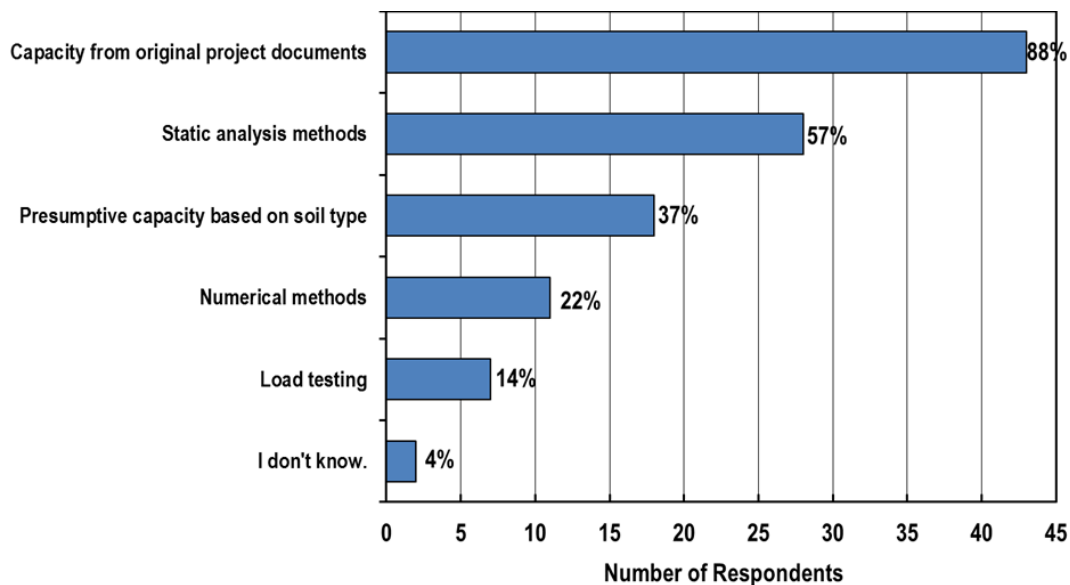
Figure 5: Frequency of implementing various methods of predicting load capacity of existing foundations under consideration for reuse. Results are from the survey for NCHRP Synthesis 505 (Boeckmann and Loehr, 2017). Reused with permission.

In many cases, the predicted capacity of the existing foundation system will be inadequate to safely support the new design loads, which are frequently greater than the original loads as a result of widening the existing structure and/or updating the design loads to current specifications. NCHRP Synthesis 505 and the RuFUS manual (Butcher et al., 2006) present various techniques for and examples of improving the load capacity of existing foundation systems. The most common approach is to retrofit the existing foundation systems with additional foundation elements (e.g. micropiles, driven piles, drilled shafts, tiebacks, etc.).

2.3.1   "Desk" Methods

There are several methods for predicting load capacity of an existing foundation without collecting new field data. Such "desk" methods are typically imprecise, highly variable estimates, but they are useful for preliminary evaluations of the feasibility of reuse, i.e. to determine whether performing a field investigation of the existing foundation system is worthwhile. The simplest method of predicting load capacity of an existing foundation is to use a value listed on the final plan documents from the original construction. As shown in Figure 5, the vast majority of agencies have adopted such an approach when reusing foundations. However, estimates based on old plans are typically subject to many potential errors, mainly because of a lack of clarity regarding the listed capacity values:

* The capacity values are usually design values, and the assumed factor of safety is seldom listed.
* The capacity values may actually be the design foundation load, which is derived from structural demands of the foundation rather than geotechnical capacity. In this situation, the value listed on the plans is less than the axial capacity of the foundation by at least the factor of safety, which is likely unknown, and potentially because of additional conservatism in the structural calculations.
* It may be unclear whether the value listed is the design load or capacity, in which case the uncertainties from both of the first two bullets are combined.
* Documentation of the original design calculations is commonly unavailable, in which case it is impossible to check the plan values without performing a new analysis.

Values listed on the original construction documents are therefore best used as a baseline for comparison with other predictions of load capacity. In most cases, the baseline capacity from original plan documents will be lower than other predictions because of the conservatism explained in the bullet points.

One method for updating the original plan document capacity is to use information from installation logs (if they are available). Illinois DOT, for example, has a procedure for updating the plan document driven pile capacity based on information regarding the pile type, pile driving installation method, and geologic information. The method is documented in NCHRP Synthesis 505. It may also be possible to perform dynamic pile capacity analysis based on the pile driving logs, but such analyses are typically imprecise, especially without reliable and specific information regarding pile driving equipment. Dynamic formulae (e.g. the Gates equation) may also be used.

After using original plan values, the second most commonly used method from Figure 5 is to perform static prediction methods, similar to the analyses that would be performed for a new foundation. However, unlike predictions for new foundations, predictions for existing foundations may be subject to additional uncertainties regarding foundation length (see Section 2.1) and other foundation characteristics (e.g. foundation element material, diameter, batter, etc.). Static prediction methods can be performed based on geologic information from the original plan documents, historical geotechnical reports, and/or historical boring logs. Although stratigraphy and material classification information from original documents may be reliable, the historical survey datum may be different from current datum, which results in differences in layer elevations. In addition, historical standard penetration test (SPT) blow count values are often unreliable, especially when the hammer efficiency is unknown. The historical blow counts are typically from hammers that were less efficient than their modern counterparts, which results in unconservative designs. Because of these potential inaccuracies, it is prudent to perform additional subsurface investigations to confirm and supplement historical information prior to proceeding with foundation reuse.

2.3.2   Field Load Tests

Performing field load tests of existing foundations is a useful method to reduce the uncertainties associated with desk predictions of load capacity. Field load tests are generally either high-strain dynamic tests (ASTM D495, 2012) or conventional static load tests, although other methods such as statnamic tests may be feasible. For both high-strain dynamic tests and conventional static load tests, there are potential efficiencies associated with foundation reuse projects that can reduce the expense of testing. High-strain dynamic tests can potentially be performed with pile driving equipment that is to be mobilized to the site for the installation of additional piles. Conventional static load tests may use the existing structure as a reaction frame if the tests are performed prior to demolition of the existing superstructure.

Field load tests of existing foundations have been implemented by seven (14%) of the agencies responding to the survey of NCHRP Synthesis 505. Field load tests are therefore less common than the desk methods, but not uncommon. Of the seven agencies, four reported using high-strain dynamic test methods, two reported using static load tests, and one reported using a test vehicle.

NCHRP Synthesis 505 documented a foundation reuse project by Maine DOT that included static load testing of existing foundations. The Haynesville Bridge superstructure replacement project was initiated in 2014. Maine DOT intended to reuse the substructure because inspection results indicated it was in good condition while the superstructure had deteriorated to poor condition. To investigate the existing timber pile foundations, MaineDOT completed four new borings, excavated test pits to expose the piles, and performed pile integrity testing, sonic echo/impulse response tests, and static load tests of two piles. The tests of the existing piles were completed by removing a 19-inch segment near the top of each pile, as shown in Figure 6(a). Static load tests were performed with axial loads applied by a hydraulic cylinder inserted where the pile segment was removed as shown in Figure 6(b). The axial load-displacement curves for each test pile are shown in Figure 7. The south abutment pile was loaded to 140 kips, more than four times greater than the original design load, without plunging. The north abutment pile plunged at 120 kips, just less than four times the original design load. The results of Figure 7 are therefore evidence of the inherent conservatism of capacity values listed on original plans. After the field tests were complete, the two ends of each test pile were re-joined by replacing the removed pile segment with cast-

in-place reinforced concrete, and the test pits were backfilled. Additional details regarding the Haynesville Bridge project are included in NCHRP Synthesis 505.
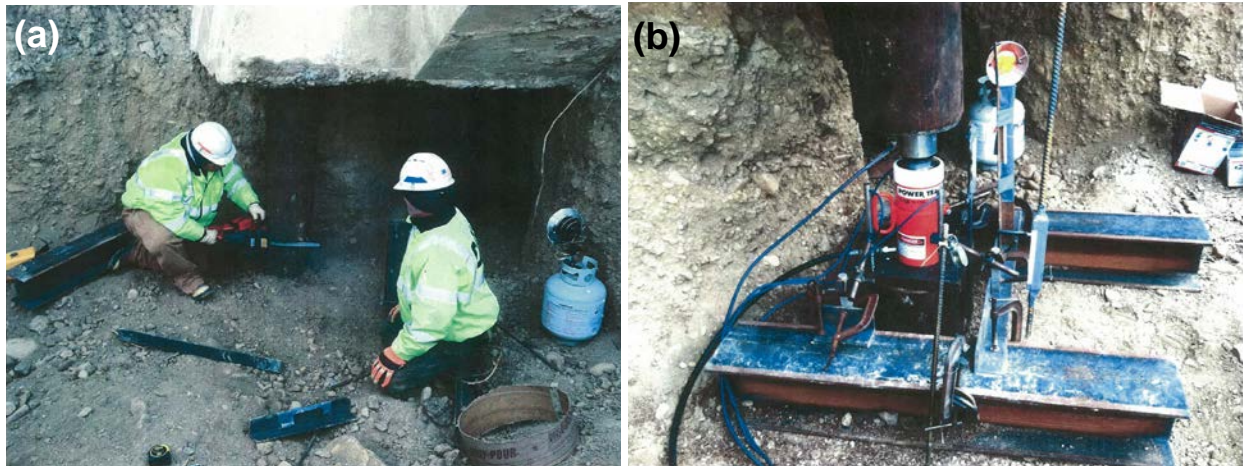
Figure 6: Field load test of timber piles for the Maine DOT Haynesville Bridge: (a) cutting timber piles to make room for (b) hydraulic cylinder used to apply load.
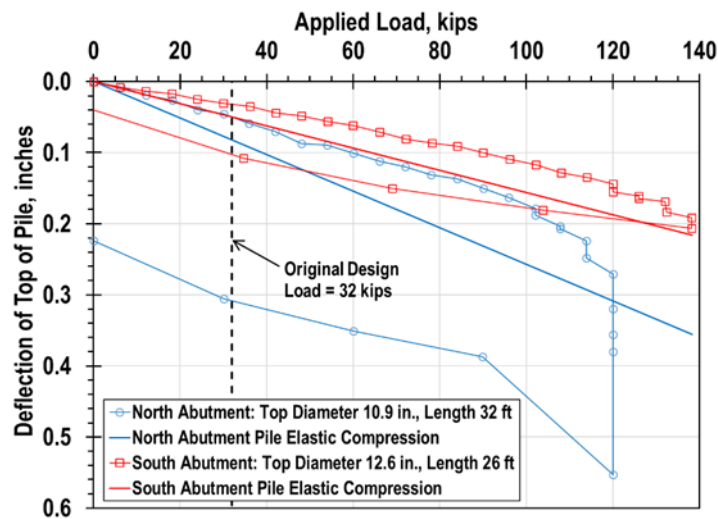
Figure 7: Axial load displacement curves for the top of test piles from the Haynesville Bridge. Results were originally presented in NCHRP Synthesis 505 (Boeckmann and Loehr, 2017). Reused with permission.

3. Methods

3.1 Test Bridges

Field measurements were performed on two low-volume bridges located on Route U and Route WW in Southeast Missouri. Both bridges were built in the 1960's and replaced in 2017. The bridges were chosen for this research study because the age of the driven piles (about 50 years) provides a useful opportunity to evaluate deterioration, the pile lengths are reasonable for exhumation, and the open access and low traffic volume at both sites make performing field test methods relatively practical. The locations and coordinates of the bridges are shown in Figure 8.
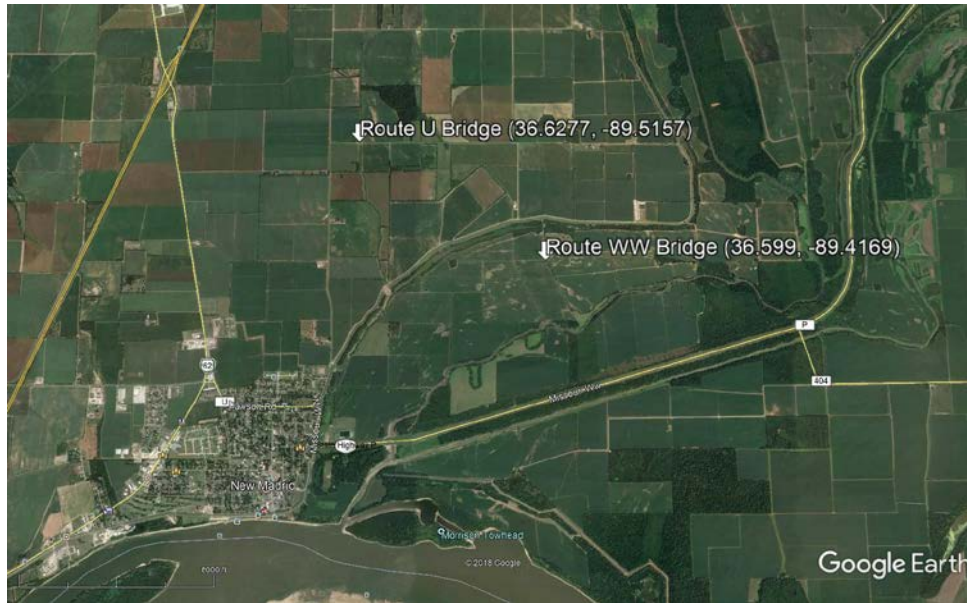
Figure 8: Google Earth image of the locations of the Route U and Route WW bridges.

3.1.1   Route U Site Description

The Route U bridge was constructed in 1967 and is located 2.9 miles northeast of New Madrid, Missouri where Route U crosses over Dry Run Ditch. The bridge is approximately 65-ft long and is supported on four bents, each consisting of four driven piles, as shown in Figure 9. A photo of the west end of the bridge prior to demolition is shown in Figure 10. The piles are precast concrete with a 16-in wide octagonal cross-section at the top. The cross section tapers significantly over the bottom 5 ft of the pile to a width of 8 in, as shown in Figure 11. Geophysical investigations were performed primarily on piles located on the west end of the bridge. The numbering convention used to identify the piles in this report is shown in Figure 9. The load test was performed on a pile on the east end of the bridge, labeled as LTP in Figure 9. Piles 1, 2, 3, 4, 6, 7 and LTP were installed with a vertical orientation. Piles 5 and 8 are battered outward from the bridge centerline, as shown in Figure 10. The slope of the batter is approximately 2 in. per foot

Borings drilled at the Route U site in January 2016 showed high plasticity, soft clays in the top 5 to 8 ft underlain by medium dense to very dense poorly graded sand to a depth of 66 ft. All historical records of the Route U site, including boring logs and CPT soundings can be found in Appendix A. Additional information collected as part of this study, including CPT logs and downhole profiles can be found in Appendix B. The downhole velocity measurements were performed by the researchers on the west end of the bridge near Pile 1. The downhole results showed shear wave velocities in the range of 490 to 890 fps over the depth range of 0 to 40 ft and saturated soil conditions below a depth of about 20 ft.
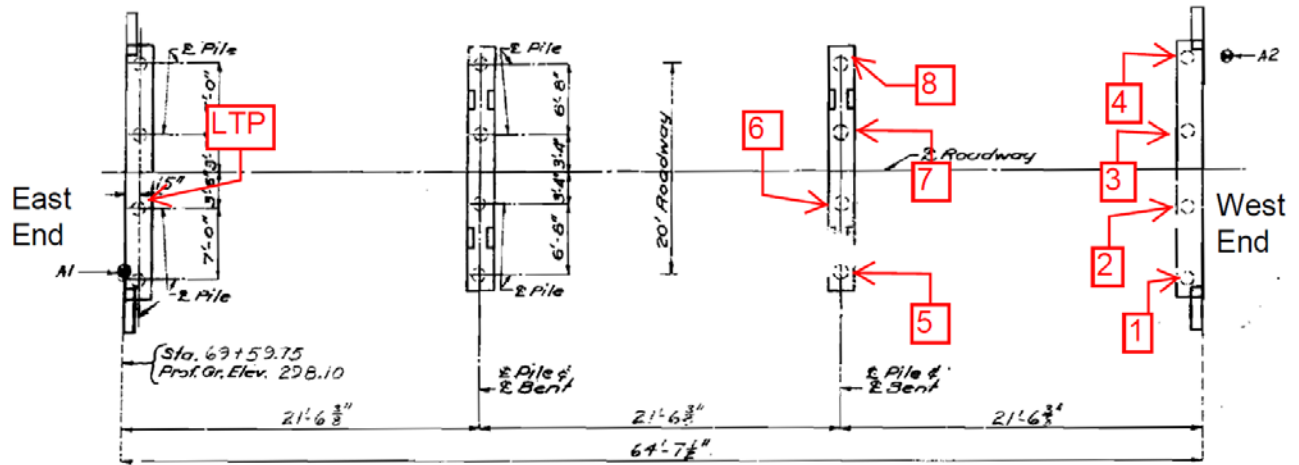
Figure 9: Pile layout and numbering used in this study for the Route U bridge with precast piles. Note that the west end bent is shown to the right and the east end bent is on the left. LTP is the load test pile.

Figure 10: Photo of west end of the Route U precast pile bridge prior to replacement.
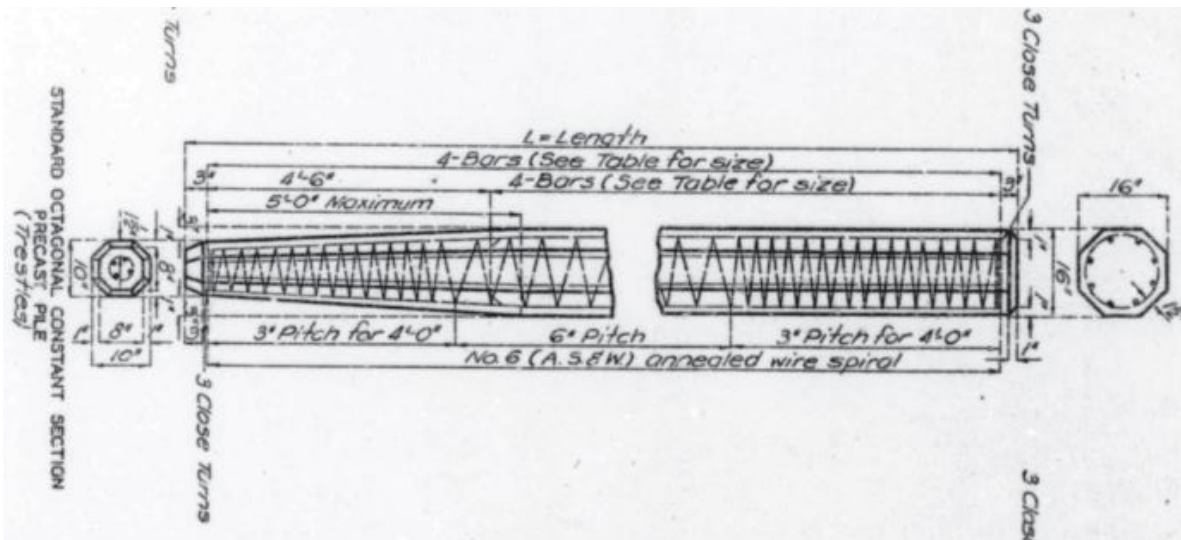
Figure 11: Plan drawing of precast pile used at the Route U site with octagonal cross-section and tapered ends over the last 5 ft.

3.1.2   Route WW Site Description

The Route WW bridge was constructed in 1968 and is located 6.5 miles northeast of New Madrid, Missouri where Route WW crosses the Wilson Bayou, as shown in Figure 8. The bridge is approximately 95-ft long and is supported on four bents, each consisting of four driven piles. The piles tested in this study are on the west end of the bridge, as shown in Figure 12. A photograph of the Route WW bridge is shown in Figure 13. The piles at this site are cast-in-place (CIP) piles, which consist of a closed-end pipe pile that is filled with unreinforced concrete after driving. The CIP piles supporting the Route WW bridge are 14-in. diameter with a nominal wall thickness of 0.25 in. A photograph of the cross section of the pile is shown in Figure 14. Piles 2, 3, 6, and 7 were oriented vertically, while Piles 1 and 4 were battered toward the abutment at 3 in. per ft and Piles 5 and 8 were battered outward from the bridge centerline at 2 in. per ft.

Based on borings and CPT measurements at this site, the general soil profile consists of soft cohesive soils overlying a dense sand layer. The depth of the dense sand layer is at about 55 ft on the west end of the bridge and increases to over 70 ft on the east end. Downhole measurements performed near Pile 1 showed shear wave velocities in the range of 450 to 550 fps to a depth of about 57 ft and shear wave velocities of about 700 fps or greater below 57 ft. Compression wave velocities indicated saturated soil conditions below a depth of about 20 ft. Details of the site geology can be found in the boring and CPT records presented for the Route WW site in Appendix A and Appendix B.
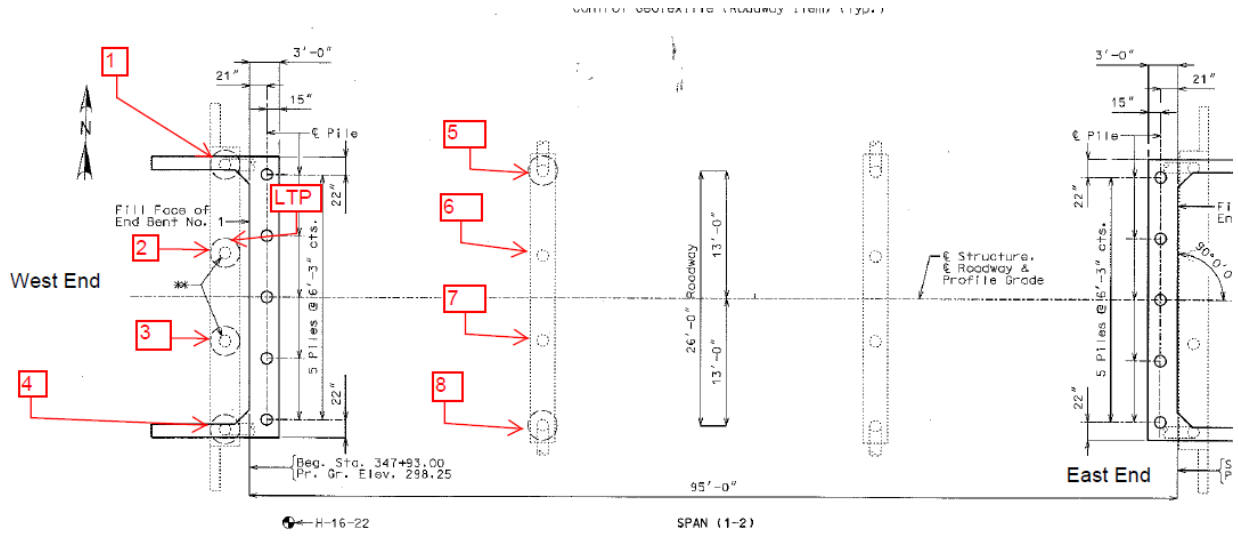
Figure 12: Pile layout and numbering used in this study for the Route WW bridge with CIP piles. All work was performed on the west end bents, as shown. LTP is the load test pile.

Figure 13: Route WW Bridge with CIP piles.

Figure 14: Concrete filled CIP pipe pile from the Route WW bridge site.

3.2   Agency Records

Pertinent MoDOT records for the bridges are included in Appendix A. The first historical document included is the MoDOT Standard Specifications for driven piles ("bearing piles") from 1961. Records for each bridge follow the specifications.

For the Route U precast pile bridge, historical records include one sheet from the final plans, four sheets of as-built ("finished") plans, a MoDOT standard sheet showing typical dimensions and reinforcement for the precast piles, and the 2016 geotechnical report for the replacement bridge. No pile driving logs were encountered for the precast pile bridge, but comparison of the final plan sheet with the first as-built sheet indicates driving of at least some of the piles was terminated at depths shallower than anticipated. The final plans called for a quantity of 405 ft of precast piles, but the as-built plans indicate a quantity of 343 ft was installed. The 2016 geotechnical report includes information from new borings and CPT soundings as well as MoDOT's predicted pile capacity values for new piles.

Historical records for the Route WW CIP pile bridge include final plans, one sheet of as-built plans (stamped "finished" as shown in the appendix), a MoDOT standards sheet from 1962 detailing CIP piles, a record of pile driving, historical boring logs, and the 2016 MoDOT geotechnical report for the replacement bridge. The single as-built sheet is a duplicate of the first sheet from the final plans; the sheet number listed on the as-built sheet is "1A of 1," which indicates it is the only as-built record. Notably, the pile driving record sheet was not discovered until the district-level personnel searched for it in preparation for driving piles for the replacement bridge; previous efforts to locate the driving records by central office geotechnical engineers were unsuccessful. The difficulty of locating such records is not surprising, nor is the fact that district level personnel succeeded where central office personnel could not, since the records were housed in the district office. These facts suggest a useful lesson regarding coordination among headquarters and district-level engineers, and perhaps also regarding the value of persistence when it comes to searching for 50-year-old records. These lessons are almost certainly not unique to MoDOT.

The as-built sheet lists a quantity of 1,034 ft for CIP piles, compared to 1,020 ft on the final plans. The relatively small difference corresponds with the installed lengths from the pile driving record sheet; the recorded installation lengths are all relatively consistent with planned lengths. The pile driving record sheet also includes information from the end of pile driving for each pile: number of blows, stroke of the hammer ram, average penetration, and the corresponding pile "bearing," presumably from dynamic formula calculations. The 2016 geotechnical report includes information from new borings, CPT soundings, and laboratory tests as well as MoDOT's predicted pile capacity values for new piles.

3.3   Geophysical Investigation Data Collection

The geophysical techniques used in this study were: (1) Parallel Seismic (PS) prior to bridge demolition using a seismic cone penetrometer (SCPT) as the receiver (2) Parallel Seismic (PS) prior to bridge demolition using boreholes installed at the site and a three-component downhole sensor as the receiver (3) Sonic-Echo (SE) measurements performed prior to bridge demolition with side-mounted geophones (4) Sonic-Echo (SE) and Impulse Response (IR) performed after removal of the superstructure with a top-mounted geophone (5) Direct velocity measurements on exposed sections of piles before removal and (6) Direct velocity measurements on exhumed piles. The data collection methods used for each of these measurements are presented below. Data interpretation methods are presented in the following section.

3.3.1   Parallel Seismic Data Collection using the MoDOT SCPT Rig

Parallel seismic measurements were performed at the Route U site and the Route WW site on Dec. 13, 2016 and Dec 22, 2016, respectively. The measurements were performed by MoDOT personnel, led by Paul Hilchen formerly of MoDOT.

Four SCPT soundings were performed as part of this study at the Route U bridge site with precast piles. The cone resistance values obtained from these soundings are presented in Appendix B. These soundings are labelled as H-16-71, H-16-72, H-16-73 and H-16-74 in Figure 15 and the elevations of each sounding are presented in Table 1. H-16-71 was used to record wave arrivals from Pile 1 and Pile 2, H-16-72 was used to record wave arrivals from Pile 3 and Pile 4, H-16-73 was used to record wave arrivals from Pile 8, and H-16-74 was used to record wave arrivals from Pile 5. The distance between the SCPT locations and the piles at Route U are presented in Table 2. The SCPT rig was positioned over the locations shown in Figure 16a, and the cone was pushed into the ground with measurements performed at depth increments of 3.28 ft (1 m), typically. To collect data at each depth increment, the rig was turned off to reduce ground vibrations and the bridge deck was impacted vertically above the pile of interest using a 12-lb sledge hammer source, as shown in Figure 16b. The sledge hammer source impacted a metal plate which closed an electrical trigger circuit to start the recording. For soundings H-16-71 and H-16-72, the locations above the adjacent piles were also impacted and recorded before advancing the cone. The seismic energy radiating from the piles was detected with the horizontally oriented geophones in the SCPT and recorded by the SCPT data acquisition system using a sampling frequency of 25,000 Hz. The SCPT probe did not include a vertically oriented geophone, so no records of vertical motion were collected. After completion of measurements at a given depth increment, the rig was turned back on and the SCPT was advanced to the next depth increment. The time records from this site were supplied to the MU researchers for interpretation and analysis.

The same general procedure was used at the Route WW site with CIP piles. Four soundings, labeled as H-16-75, H-16-76, H-16-77, and H-16-78 were advanced at this site, as shown in Figure 17. The elevations of each of the soundings are presented in Table 3. The distance between the SCPT locations and the piles at Route WW are presented in Table 4. At this site it was not possible to locate the SCPT soundings close to the piles of interest, so distances between the SCPT and piles were larger than at the Route U site. Also, due to the longer expected pile lengths at this site, the penetration depth of interest was greater. In some cases, the capacity of the rig was insufficient to penetrate the dense sand layer and the sounding was terminated at a depth that did not allow for determination of the pile length.
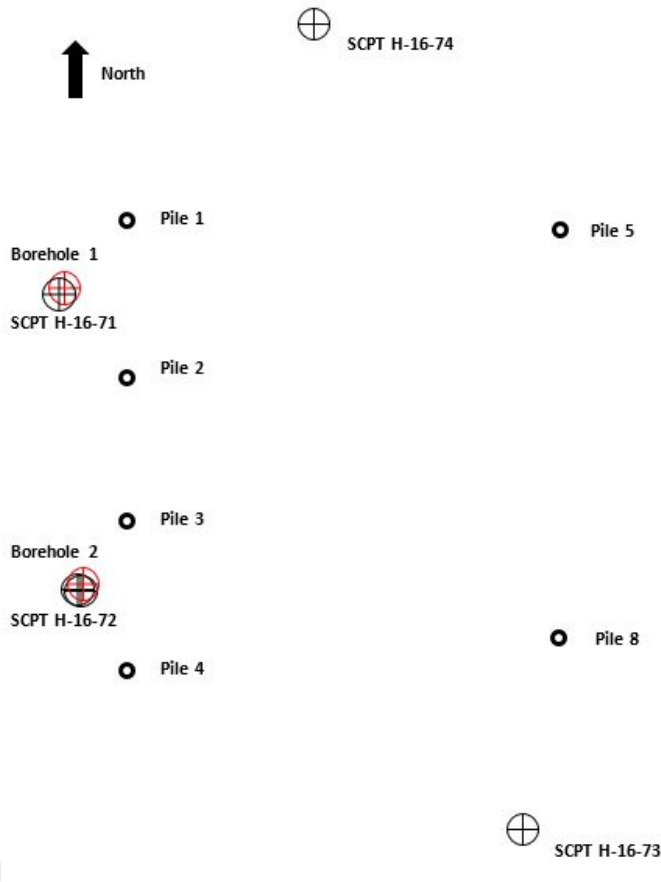
Figure 15: SCPT, borehole and precast pile locations at the Route U bridge site.

Table 1: Surface elevations of boreholes and SCPT soundings at Route U site (precast piles).

	BH 1	BH 2	SCPT H-16-71	SCPT H-16-72	SCPT H-16-73	SCPT H-16-74
Elevation (ft)	298.1	298.1	298.1	298.1	290.6	293.3

Table 2: Distance from boreholes and SCPT locations to piles tested at Route U (precast piles).

Pile Number	Distance from Pile to Borehole / Sounding (ft)					
	BH 1	BH 2	SCPT H-16-71	SCPT H-16-72	SCPT H-16-73	SCPT H-16-74
1	4.8	17.8	6.3	-	-	-
2	4.9	10.7	5.0	-	-	-
3	11.4	4.1	-	4.0	-	-
4	17.8	4.1	-	5.3	-	-
5	-	-	-	-	-	15.6
8	-	-	-	-	8.8	-

Figure 16: PS testing at the Route U bridge site: (a) SCPT rig and (b) impact hammer.
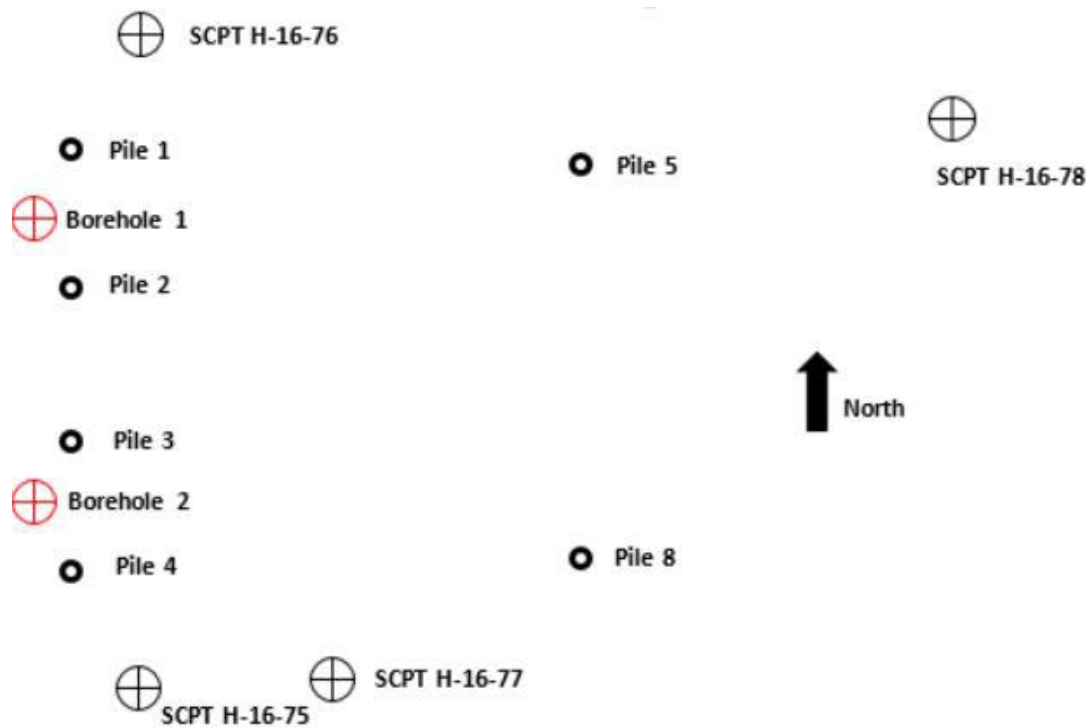
Figure 17: SCPT, borehole and CIP pile locations at Route WW site.

Table 3: Surface elevations of boreholes and SCPT soundings at Route WW site (CIP piles).

	BH 1	BH 2	SCPT H-16-75	SCPT H-16-76	SCPT H-16-77	SCPT H-16-78
Elevation (ft)	298.5	298.5	293.5	293.6	291.2	280.5

Table 4: Distance from boreholes and SCPT locations to piles tested at Route WW (CIP piles).

Pile Number	Distance from Pile to Borehole / Sounding (ft)					
	BH 1	BH 2	SCPT H-16-75	SCPT H-16-76	SCPT H-16-77	SCPT H-16-78
1	4.8	22.6	-	9.2	-	-
2	4.1	13.8	-	17.5	-	-
3	13.8	5.1	16.6	-	-	-
4	22.9	5.3	8.3	-	-	-
5	34.9	-	-	-	-	24.5
8	34.9	34.9	-	-	18.3	-

3.3.2   Parallel Seismic Data Collection using Borehole Sensors

Parallel seismic measurements were performed at the Route U site (precast piles) on February 8 and 9, 2017. Two 2.5-in. diameter, flush-joint, PVC-cased boreholes were installed and grouted at the site by MoDOT personnel in December 2016. The locations of the parallel seismic boreholes were shown in Figure 15. The elevations of the boreholes and distance between the boreholes and the piles were presented in Table 1 and Table 2, respectively. Each borehole was bailed by hand prior to testing so that measurements could be performed in a dry casing. A three-component geophone downhole sensor manufactured by GeoStuff (shown in Figure 18a) was used as the receiver for these measurements, whereas sensors on the SCPT rig were used as the receiver for the measurements described in the previous section. Instrumented sledge hammers, Models 086D20 (3-lb) and 086D50 (12-lb) manufactured by PCB Piezotronics, were used as impact sources, as shown in Figure 18b. The measurements were performed by lowering the sensor to the depth of interest and locking the sensor again the borehole. A downhole servo motor on the borehole device was actuated to orient the horizontal sensors in-line with the pile locations. Impacts were then performed on the roadway above the location of each of the piles to be tested. Recordings were taken from the source impact using both horizontal sensors and the vertical sensor. Typically, three to five impacts were stacked at each location to improve the data quality. The data were recorded using a Data Physics "Quattro" four-channel signal analyzer using a sampling frequency of 25,600 Hz. After completion of all recordings at a given depth, the borehole sensor was released and lowered to the next depth. Measurements were performed until the sensor reached the bottom of the borehole.

Measurements at Route WW (CIP piles) were performed from the Borehole 2 location on February 9, 2017 and from the Borehole 1 location on February 22, 2017. Borehole installation and testing procedures were the same as described above for the Route U location. The locations of the boreholes are shown in Figure 17, with elevations and distances to piles presented in Table 3 and Table 4, respectively.

Figure 18: Parallel Seismic equipment used: (a) three-component downhole sensor (shown next to Borehole 2) and (2) instrumented sledge hammer (impacting over Pile 2 location).

3.3.3   Sonic Echo (SE) Measurements Performed Prior to Bridge Removal

Sonic Echo (SE) measurements were performed on July 3, 2017 at the Route U and Route WW sites prior to the removal of the bridge deck. The sides of end bent piles (Piles 1 through 4 at both sites) were buried and therefore not accessible for the SE-IR measurements. Therefore, measurements were performed on Piles 7 and 8 at both the Route U (precast piles) and Route WW (CIP piles) sites. To perform these measurements, two 28-Hz geophones were coupled to the side of the pile using large hose clamps, as shown in Figure 19. At Route U the geophones were separated by 1.67 ft on Pile 7 and 1.25 ft on Pile 8. At Route WW they were separated by 3.0 ft on both Pile 7 and Pile 8. Energy was excited in the pile by impacting the bent at the top of the pile or by initiating a glancing blow along the side of the pile.

The time domain SE data were recorded using the Data Physics 4-channel signal analyzer with a sampling frequency of 102 kHz to ensure good resolution in the time domain.

Figure 19: SE test setup on precast Pile 7 at the Route U site.

3.3.4   Sonic Echo (SE) and Impulse Response (IR) Measurements Performed after Removal of Bridge

Sonic Echo and Impulse Response tests were performed on: (1) July 12 and 13, 2017 on the piles used for the load tests at the Route U and Route WW sites, (2) on July 18, 2017 for the other CIP piles at the Route WW site and (3) on July 27, 2017 on the remaining precast piles at the Route U site. After the bridge superstructure was removed, the tops of test piles were cut by the contractor to produce a flat and smooth surface. A photograph of the Route U site after the piles had been prepared is shown in Figure 20. Elevations of the cut pile surfaces are presented in Table 5 and Table 6 for Route U and Route WW, respectively. Vibrations were detected using a 28-Hz geophone which was epoxied to the surface of the pile, as shown in Figure 21. At the Route U site, a piezoelectric accelerometer was also used to allow for comparisons of the results obtained using different sensor types. The geophone and the accelerometer showed nearly identical results, so only data collected with the geophones are presented in this report. Energy was excited using a vertical impact from a 3-lb (PCB 086D20) instrumented sledge hammer. The time domain SE data were recorded using the Data Physics 4-channel signal analyzer with a sampling frequency of 102 kHz to ensure good resolution in the time domain. The IR frequency domain data were recorded with a slower sampling frequency of 5120 Hz to produce better frequency domain resolution.

Figure 20: Overview photo of Route U site after bridge was removed and precast piles were cut.
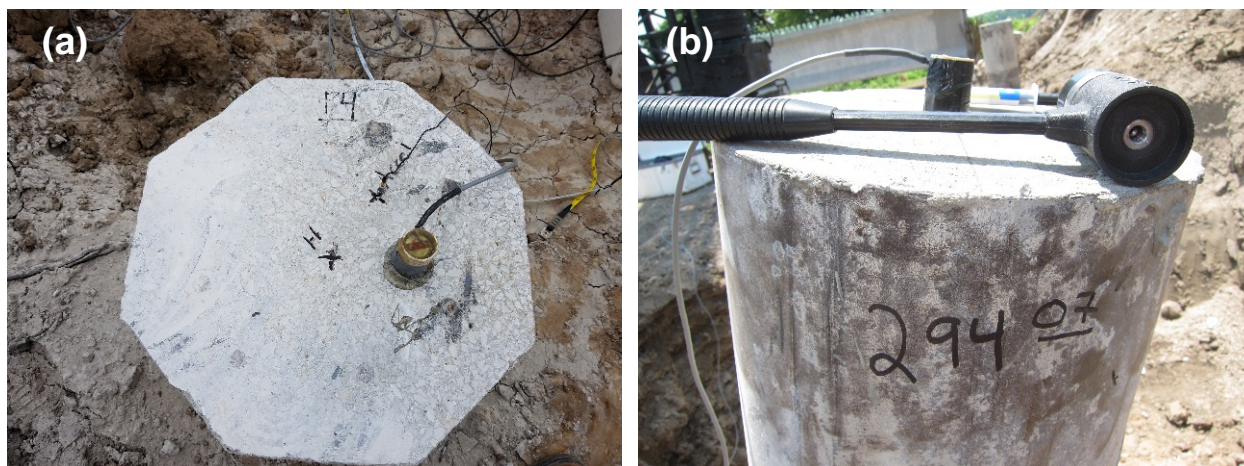
Figure 21: Test setup for SE-IR after removal of bridge deck at (a) Route U (precast pile) and (b) Route WW (CIP pile).

Table 5: Route U precast pile cutoff elevations.

	Pile 1	Pile 2	Pile 3	Pile 4	Pile 5	Pile 6	Pile 7	Pile 8	LTP
Elevation (ft)	292.51	294.02	-	292.43	293.64	293.69	293.60	292.66	290.22

Table 6: Route WW CIP pile cutoff elevations.

	Pile 1	Pile 2	Pile 3	Pile 4	Pile 5	Pile 8
Elevation (ft)	294.07	290.00	294.34	293.79	294.42	294.45

3.3.5   Direct Velocity Measurement of In-place Piles

Measurements of compression wave velocity were made in the exposed portion of selected piles at the Route U (precast piles) and Route WW (CIP piles). The measurements were performed on the piles after the bridge was removed. Two 28-Hz geophones were clamped to the sides of the exposed portion of the pile. The surface of the pile was impacted with an instrumented hammer and the time records were recorded using the Data Physics analyzer with a sampling frequency of 100 kHz. Direct velocity measurements were made on Pile 6 at Route U and on Pile 3 at Route WW.

3.3.6   Direct Velocity Measurements of Exhumed Piles

Direct measurements of compression wave velocity were also performed on the exhumed piles from each site. To perform these measurements, 28-Hz geophones were clamped to the side of the pile and compression wave energy was excited by striking the end of the pile with an instrumented hammer. For the Route U precast piles, a single geophone was placed at approximately the mid-length of the pile. For the CIP piles at Route WW, which are significantly longer than the Route U precast piles, geophones were placed at multiple locations along the pile. The locations corresponded to distance intervals ranging from 12 to 45 ft. The experimental set-up for the testing of the exhumed CIP piles from Route WW is shown in Figure 22.

Figure 22: Experimental setup for measuring wave velocities in exhumed CIP piles at Route WW.

3.4 **Geophysical Data Interpretation**

3.4.1 Interpretation of Parallel Seismic Data

Parallel seismic data collected in the field were downloaded from the recording devices and uploaded into the program IGOR by Wavemetrics. Each time record was normalized (divided by its maximum value) and plotted versus depth, as shown in Figure 23. The arrivals of compression wave energy radiating from the pile (termed p-p for p-wave in the pile and p-wave in the soil) and shear waves radiating from the pile (termed p-s for p-wave in the pile and s-wave in the soil) were picked manually by identifying the first break in the record. The wave arrivals for precast Pile 2 at Route U are shown in Figure 23. Two approaches were used for interpreting the Parallel Seismic data. In the primary approach, travel time equations were written and an iterative curve fitting procedure was implemented in IGOR to search for the best fitting values of compression wave velocity of the pile, soil velocity (both shear and compression waves), and length of the pile. Velocity values were constrained to fall within the range of 11,500 to 14,000 fps for compression waves. This model assumed uniform soil conditions (no change in velocity with depth). An example of the output of this curve fitting procedure using the data for precast Pile 2 from Route U (i.e. using the data from Figure 23) is shown in Figure 24. Data collected above the water table were not included in the fit due to significant variability caused by non-saturated conditions. Below the water table, compression wave velocities in the soil are consistently around 5000 fps.

A secondary approach was implemented for cases where the model solution could not be used due to complicated geometries from battered piles or non-convergence of the solution. For these cases, the traditional approach of finding the intersection of the bilinear sections was used to estimate the depth of the pile tip. In some cases, such as long offset distances between the pile and the borehole/SCPT it was not possible to identify a break in the arrival time plots or unreasonable travel times were recorded. In these cases, the results were reported as ND (not determined).
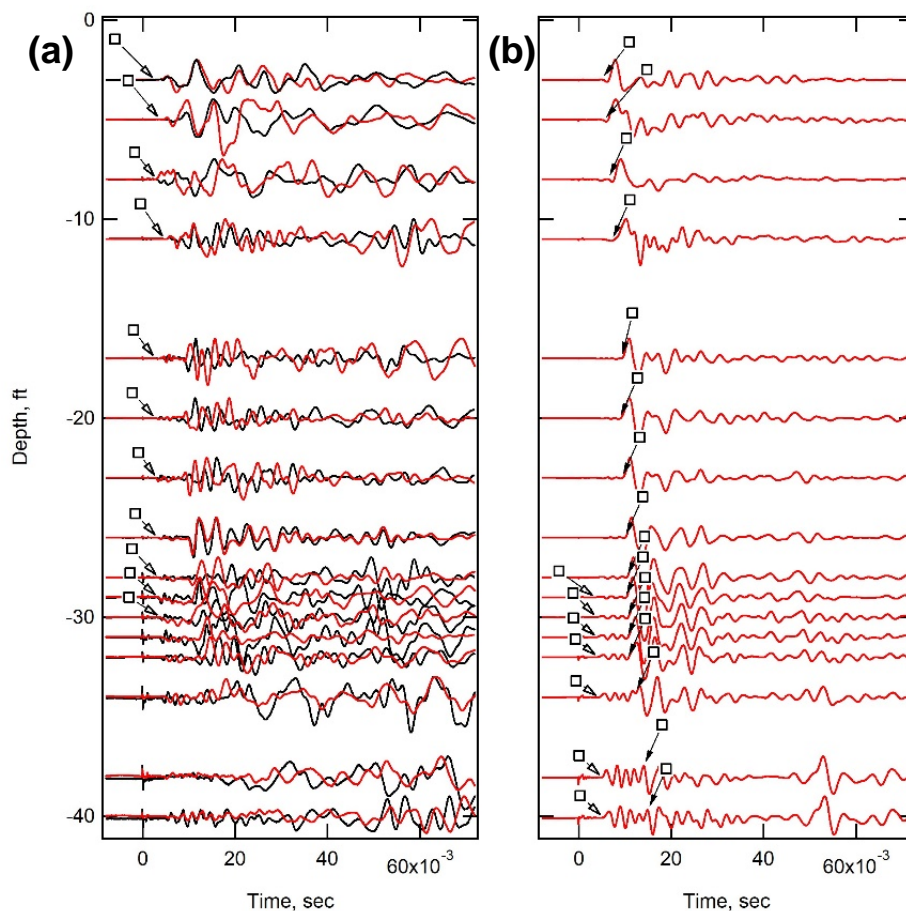
Figure 23 Example showing picks of compression wave arrivals (open arrows) and shear wave arrivals (closed arrows) from Parallel Seismic testing on precast Pile 2 at Route U site recorded on the horizontal geophones (left) and vertical geophones (right).
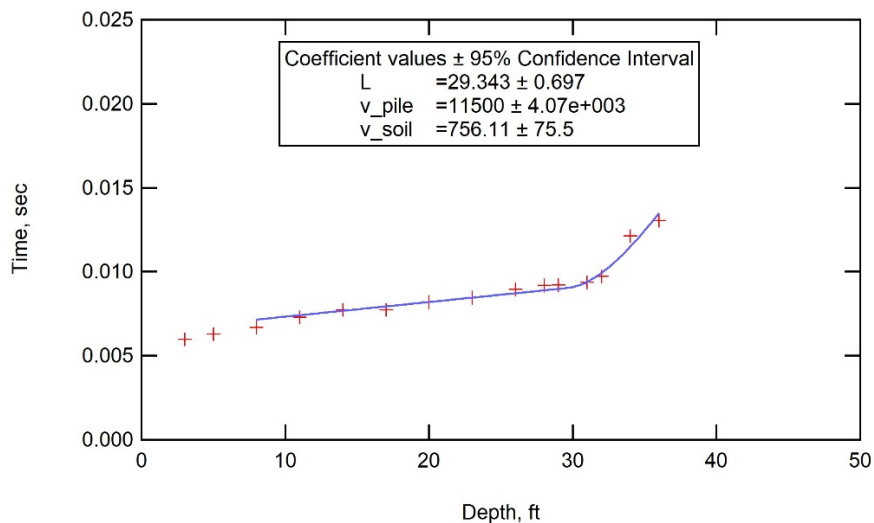
Figure 24 Example of the model fit to p-s wave arrivals from BH1 to precast Pile 2 at Route U.

3.4.2   Interpretation of Sonic Echo (SE) Data

Time domain records collected from SE measurements were downloaded from the Data Physics software and input into the program IGOR. Plots of the recorded source impact and recorded geophone response were used to manually pick the source impact time and the arrival time of the reflections from the base of the pile, as shown in Figure 25. The time difference between the arrivals (t) along with the compression wave velocity of the pile (V) was used to calculate the pile length (L) using:

$$L = \frac{V \times t}{2} \tag{1}$$

The compression wave velocity of the pile is one of the unknowns in this equation and must be either measured or assumed. For this work the velocities from the direct wave measurements were used to determine the length. The variability in the direct velocity measurement from in-place and exhumed piles is discussed in the Chapter 4.
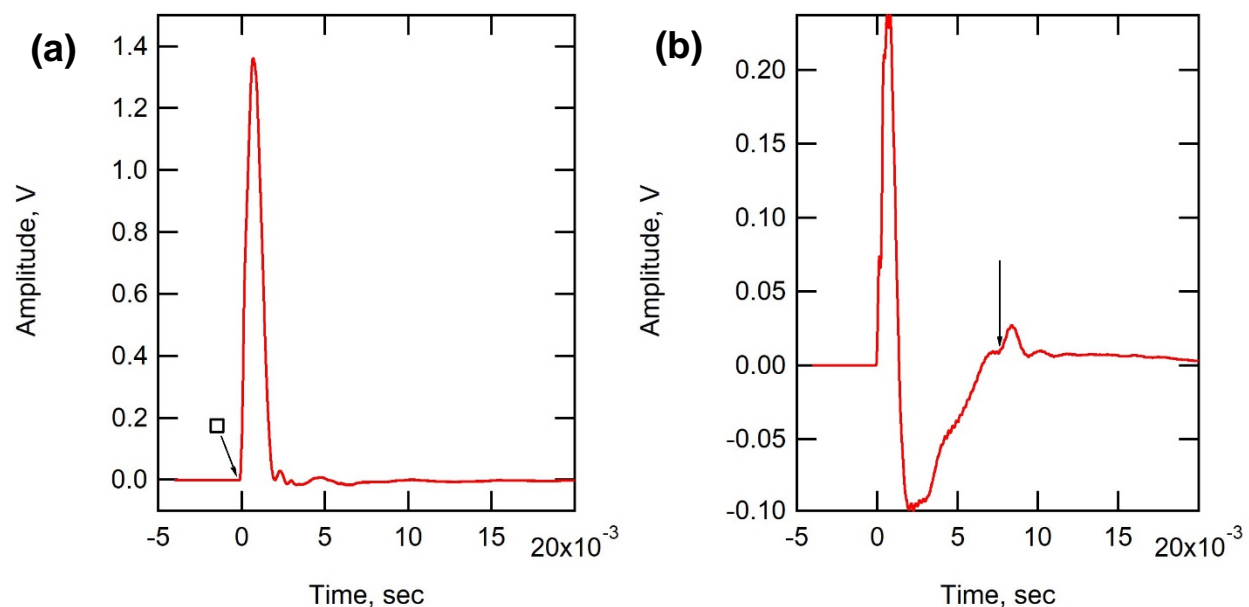
Figure 25: Example SE records from CIP Pile 2 at Route WW showing times of (a) impact and (b) reflected arrival.

3.4.3   Interpretation of Impulse Response Data

Frequency domain data from the source and receiver were exported from the Data Physics program and loaded into IGOR. The ratio between the frequency spectrum of the receiver and the frequency spectrum of the source was calculated, as shown in Figure 26. The length of the pile (L) can be calculated from the frequency span between peaks in the IR record (f) and the velocity of the pile from:

$$L = \frac{V}{2 \times f} \tag{2}$$

When multiple peaks were evident in the figure the average span was used to calculate the length.
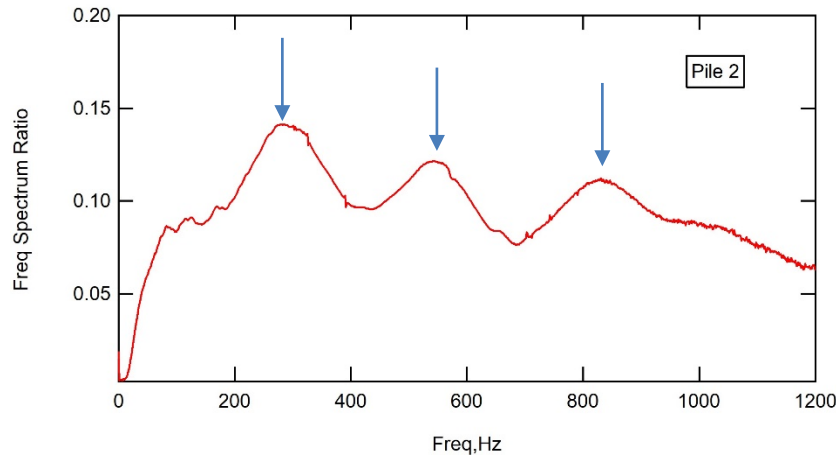
Figure 26: Example Impulse-Response records from precast Pile 2 at Route U.

3.4.4   Interpretation of Direct Arrival Data

The direct wave arrival data were used to measure compression wave velocities in the exhumed piles from Route U (precast piles) and Route WW (CIP piles). The time record data were uploaded in IGOR and the time of arrival of the wave at each geophone was picked manually from the records. The velocity was calculated from the spacing between receivers (d) and the time between arrivals as:

$$V = \frac{d}{t} \tag{3}$$

At Route U, velocity values were calculated from the bottom of the pile to the mid-length geophone and from the top of the pile to the mid-length geophone. The average velocity was calculated from the travel time over the whole pile length and was used in the calculation of length for the SE and IR methods. At Route WW, three or four interval velocity measurements were calculated and the velocity from the longest measured interval was used in the calculation of pile length for the SE and IR methods.

3.5   Prediction of Load Capacity by Static Methods

Various static (aka "rational") methods were used to predict the capacity of the existing precast and CIP piles. The predictions serve two purposes: (1) inform the load test preparations (see Section 3.6) and (2) provide capacity values for comparison with load test results (see Chapter 4). The results are summarized in Table 7 for precast piles and Table 8 for CIP piles. Calculations documenting the University predictions are presented in Appendix C, except for the Eslami and Fellenius method results, which are presented in Akkus (2018). The MoDOT predictions are presented in the geotechnical reports included in Appendix A. The MoDOT predictions were made for driven pile types that are not necessarily the same size and shape as the existing piles. The predictions presented in Table 7 and Table 8 are therefore based on the unit side and end resistance values assumed by MoDOT but applied to the existing piles.

Table 7: Predicted axial pile capacity values from static method analyses of precast piles.

Method	Predicted Capacity, kips		Notes
	Compression	Uplift	
Value from historical plans	28 or 42	N/A	Two values listed in plans: "computed capacity" (28 kips) and "plan capacity" (42 kips). Values are likely allowable.
Static predictions (University):			All values ultimate.
Eslami and Fellenius	280		From Akkus (2018)
Meyerhoff (SPT)	N/A	35	
Brown (SPT)	130	64	
Alpha / Nordlund (MU)	574	N/A	Only method to account for taper.
Static prediction (MoDOT):			Ultimate values. Results reported in MoDOT's 2016 geotechnical report for replacement bridge. Values are scaled from unit side and end resistance values for larger piles.
LCPC (CPT)	110	56	
Alpha / Nordlund	106	41	

Table 8: Predicted axial pile capacity values from various analyses of CIP piles.

Method	Predicted Capacity, kips		Notes
	Compression	Uplift	
Value from historical plans	60	N/A	Allowable value with unknown factor of safety.
Values from pile driving record (dynamic formulas):			Allowable values; FS = 6?
Range (all piles)	60 to 115	N/A	
Test pile	67 or 83	N/A	Not clear whether test pile was Pile 2 or Pile 3
Static predictions (University):			All values ultimate. Calculations documented in Appendix C, except for Eslami and Fellenius, which is documented in AKKUS (2018).
Eslami and Fellenius	230		
Meyerhoff (SPT)	213	43	
Brown (SPT)	346	211	
Alpha / Nordlund	334	174	
Static prediction (MoDOT):			Ultimate values. Results reported in MoDOT's 2016 geotechnical report for replacement bridge. Values are scaled from unit side and end resistance values for larger piles.
LCPC (CPT)	335	85	
Alpha / Nordlund	480	200	

For the precast piles, the historical plan documents list a "plan capacity" of 21 tons (42 kips) and a "computed capacity" of 14 tons (28 kips). Definitions of these terms were not encountered in any of the historical MoDOT documentation, but comparison with the values predicted by static methods indicates the historical plan values are likely allowable, but again with an unknown factor of safety. The static prediction values range from 110 to 574 kips in compression and 35 to 64 kips in uplift. The 574-kip estimate is based on the University's prediction with the Nordlund method, and is the only value to consider the taper of the precast piles, which significantly increases the geotechnical resistance in compression. The predictions in the MoDOT geotechnical report were for pipe piles. The results in the report were divided by pile area to calculate unit resistance values, which were then applied to the presumed area of the precast piles. The unit resistance values from the MoDOT report do not account for taper.

For the CIP piles, the historical plans list a "design bearing" of 30 tons. Presumably the design value includes a factor of safety, but it is unclear what specific value of factor of safety was employed. The 1961 MoDOT specifications require use of dynamic formulas to confirm capacity using penetration data from the end of driving. Values from the dynamic formula were included on the pile driving record (Appendix A), and are summarized in Table 8. According to the specifications, use of the formulas produces a "safe allowable bearing value," but the factor of safety is again unspecified. The formulas are equivalent to the ENR formula that was frequently employed at the time of construction (and unfortunately is still in use today). The ENR formula purportedly includes a factor of safety of 6.

Multiplication of the dynamic formula results in Table 8 by a factor of six produces ultimate values that are mostly within the range of values predicted by static methods. As shown in the table, the static predictions range from 213 to 346 kips in compression, and 43 to 211 kips in uplift. The predictions are based on a variety of static methods, and make use of historical boring information (unconfined compression tests), new cone penetration test (CPT) data, and new standard penetration test (SPT) data. Also listed in the table are the results of a static prediction by MoDOT for new 14-inch pipe piles (i.e. equivalent to the existing piles). MoDOT's predicted value was based on the alpha method in the clay along most of the pile length and Nordlund's method for the portion of the pile embedded in sand near the pile tip. The capacity values predicted by MoDOT are different from those predicted by the University for the same methods (alpha and Nordlund), which is unsurprising given the sensitivity of the static predictions to assumed material properties and the variability of those properties from the various subsurface investigations. Overall, the static predictions of the capacity of both types of existing piles include significant variation, but all are significantly greater than the design values listed on the historical documentation.

3.6   Load Tests

One pile was selected at each bridge for axial load testing. The load test plan involved using the existing bridge as the reaction frame for the test pile, similar to the arrangement employed by Maine DOT for the Haynesville Bridge project described in Section 2.3.2 and shown in Figure 6. Accordingly, end bent piles were selected as the test piles. Within the end bent, interior piles (i.e. toward the centerline of the roadway) were selected for testing since the outside piles were battered, and to produce a more favorable distribution of bending moments and shear forces within the existing capping beam to be used as the reaction. Structural analysis indicated the shear and bending moment capacities of the capping beams could be limiting factors (i.e. the beam could break at loads less than the geotechnical resistance of the test pile), but the capacity of the existing capping beam was estimated to at least be greater than the design values from the historical plan documents. Another potential limiting factor was uplift capacity of the piles adjacent to the test pile; these piles serve to anchor the capping beam during the test. The potential for uplift capacity to control was more significant for the precast pile bridge, where the piles are tapered and relatively short. Despite these potential imitations, the option of using the existing capping beam as the reaction was selected over building a new reaction frame to reduce costs, reduce schedule impacts, and provide practical lessons for future load tests of existing piles using the existing bridge as a reaction.

To apply the test load, an approximately 15-in. long segment of each test pile was removed to create space for a hydraulic cylinder as shown in Figure 27. Prior to testing, the 200-ton hydraulic cylinder was calibrated; results of the calibration are shown in Figure 28. The calibration results were used to indicate the applied load during testing from measurements of hydraulic pressure. Photographs of the load tests are shown in Figure 29 for the precast pile and Figure 30 for the CIP pile. The photographs show steel bearing plates used to distribute load from the hydraulic cylinder to the ends of the piles. The photographs also show a dial gage used to measure displacement of the top of the pile. For both tests, the base of the dial gage was affixed to the pile head and the tip of the dial gage rested against a length of steel angle section, which was welded to the sheet piling supporting the test pit excavation. The length of the angle section was between 3 and 4 ft for the precast pile load test and approximately 5 ft for the CIP pile load test. Although these reference distances are less than recommended by ASTM for axial load tests, the distances are at least three pile diameters, and it is unlikely the sheet pile walls displaced significantly as a result of the pile load test. Also shown in the photographs are vibrating wire strain gages, which were

used to provide a second set of data for load at the pile head. The axial load tests were performed incrementally. Each load increment was held until the dial gage measurements indicated the pile head movement was negligible, at which point the load was increased. The load was increased in approximately 20-kip increments. The duration of most of the loading increments was less than 10 minutes. The duration of the final two or three loading increments for each test pile was approximately 20 minutes. During the load tests, the top of the existing bridge was surveyed to monitor the response of the capping beam and potential pullout of the reaction piles.
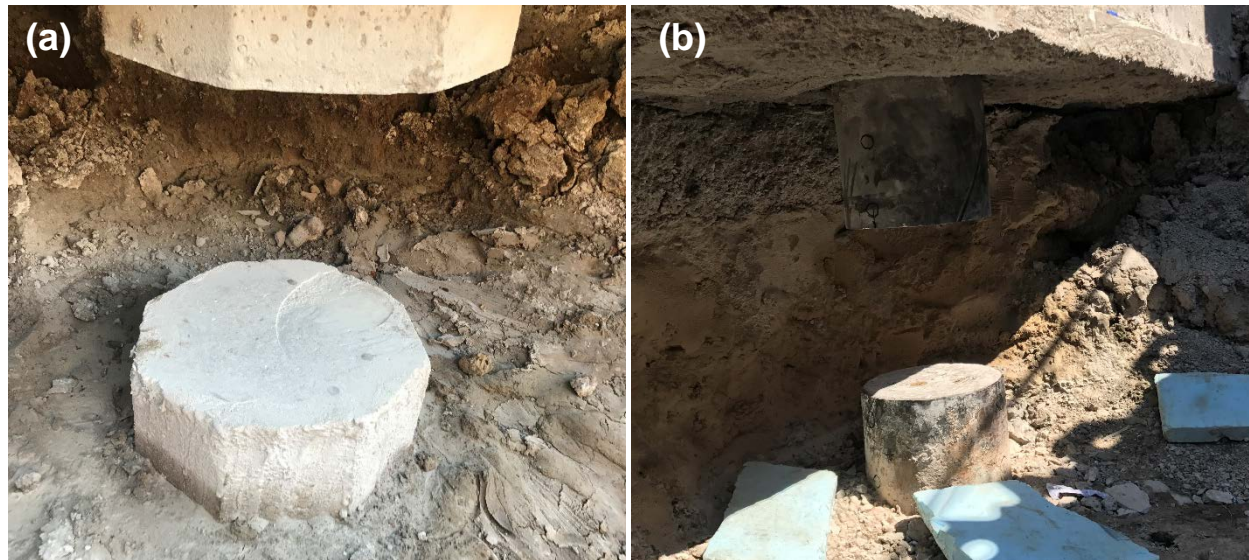
Figure 27: Test piles after removing segments to make room for hydraulic cylinder: (a) precast pile and (b) CIP pile.
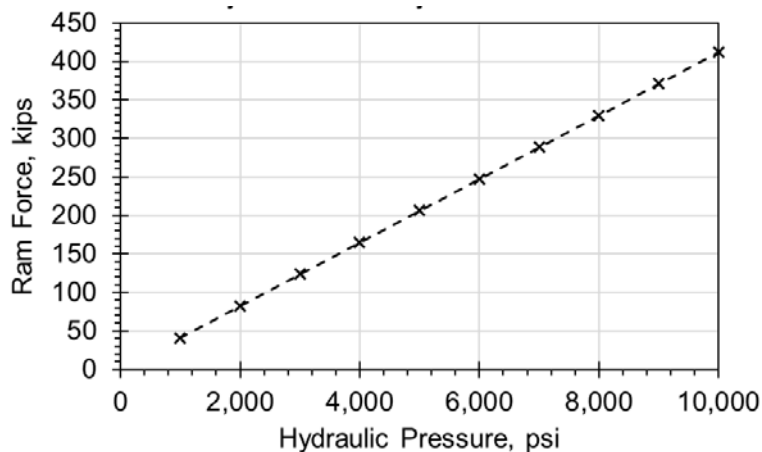
Figure 28: Calibration of hydraulic cylinder prior to load testing.
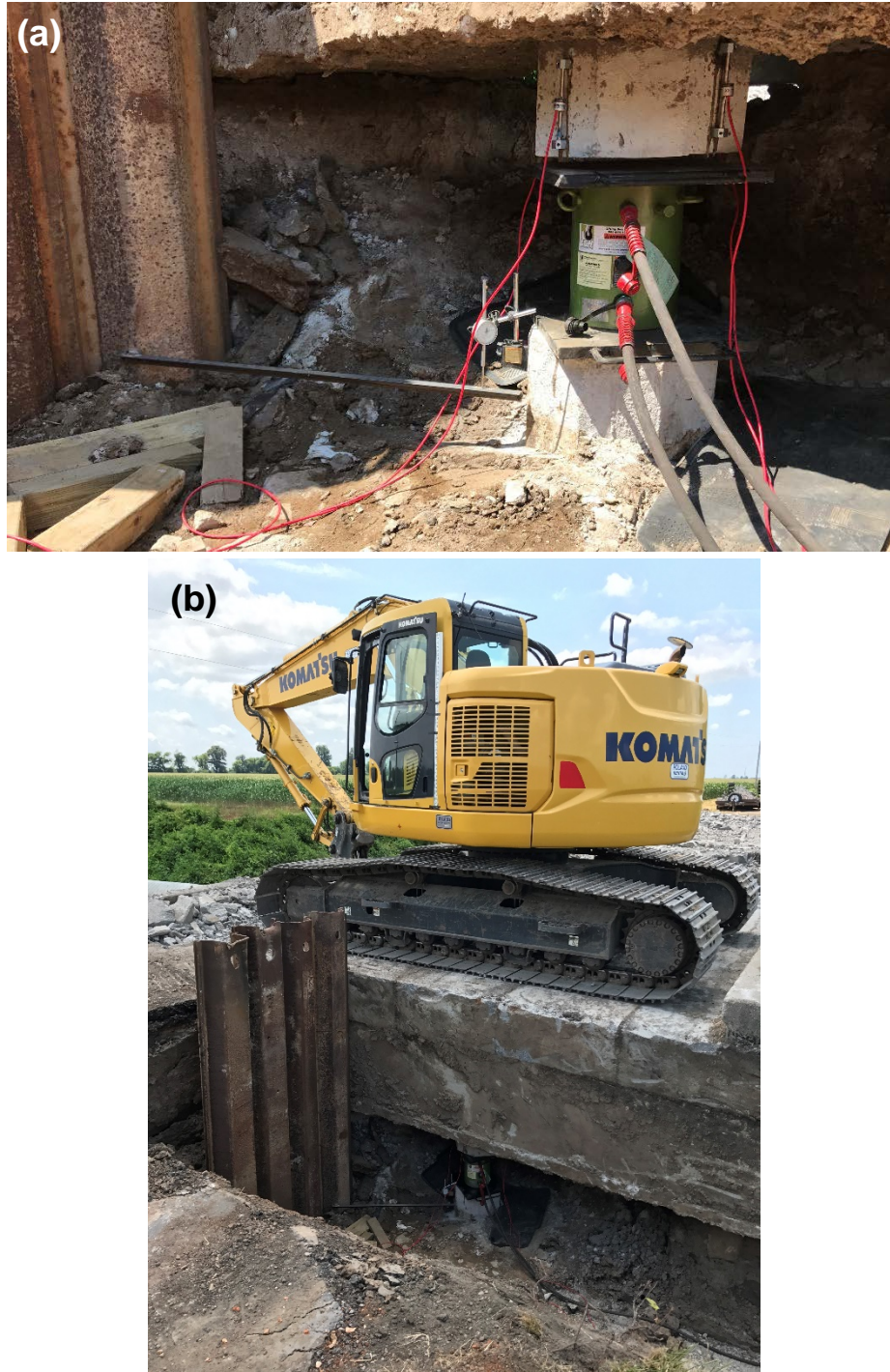
Figure 29: Photographs of load test of precast pile: (a) hydraulic cylinder applies load while strain gages are used to measure load at the top of pile and dial gage measures displacement of the top of the pile; and (b) backhoe is parked atop reaction beam to reduce loads in capping beam and reaction piles.

Figure 30: Photographs of CIP test pile load test: (a) hydraulic cylinder applies load while strain gages are used to measure load at the top of pile and dial gage measures displacement of the top of the pile; (b) view of test pile beneath existing bridge capping beam; and (c) backhoe is parked atop reaction beam to reduce loads in capping beam and reaction piles.

After the static load tests and demolition of the bridges were complete, Koehler Engineering performed dynamic pile driving analysis ("CAPWAP") of the existing piles by restriking the piles. Six piles were tested at each bridge. A photograph of one of the restrike tests at Route WW (CIP pile bridge) is shown in Figure 31. The restrikes were completed using a Delmag D-15 diesel hammer. Dynamic test data were collected using a Pile Driving Analyzer, including strain gages at the pile head. Test data were analyzed by GRL Engineers, Inc. GRL Engineers documented the tests and results in reports presented in Appendix D.

Figure 31: Restrike test of a CIP pile.

3.7   Pile Exhumation and Examination

After completion of all load tests and geophysical measurements, six piles from each site were exhumed so that inspection and measurements could be performed. The exhumed precast piles from Route U were Piles 1, 2, 4, 5, 6 and LTP. The exhumed CIP piles from Route WW were Piles 1, 2, 3, 4, 5 and 8. A photograph of Pile 1 being exhumed from the Route WW site is shown in Figure 32. The pile exhumations were observed and documented by either MoDOT personnel or MU researchers. Upon extraction the piles were marked with an identifying number and measured. Unfortunately, in some cases the numbering scheme used was different than what is used in this report, so some photos may include numbers on the piles that are not consistent with the numbering in this report. The condition of the piles was documented with photographs and the piles were laid out on blocks to allow for wave propagation

measurements. Finally, the CIP piles at the Route WW site were cut into several sections so that measurements of the pipe pile wall thickness could be performed at several depths. The wall thickness was measured with a caliper at three locations around the circumference of the pile.

Figure 32: Pile exhumation at the Route WW site.

4. Results and Discussion

Results of the experimental work described in Chapter 3 are presented in this chapter. Results regarding predictions of pile length are presented first, results regarding pile condition are presented second, and results regarding pile load capacity are presented third.

4.1   Pile Length

As discussed in Chapter 2, numerous methods can be used to predict the length of existing piles, and several different approaches were used for this project, as described in Chapter 3. Results from each method are presented in the sections below. For each method, the results are compared with true values, which were determined by exhumation of six piles from each bridge site.

4.1.1   Plans and Driving Records

Pile lengths were estimated using historical records from the original construction of the Route U and Route WW bridges. For the precast piles of Route U, only final plans and as-built plans were available (Appendix A); pile driving records were not located. Estimated quantities reported on the as-built plans showed a total length of 343 ft of driven piles for 15 installed piles. (One pile, a load test pile, was not included in the 343-ft quantity.) Based on the reported total length of driven piles, an average length of 22.9 ft per pile was estimated. Using the pile top elevation from the historical plans (second column of Table 9) and the cutoff elevation of the exhumed piles (column 3 in Table 9) the lengths estimated based on the historical records were calculated and compared to the actual exhumed lengths, as shown in Table 9. Based on this limited information, some of the piles lengths were underestimated by nearly 30%. The error in the estimates from as-built lengths is significant, perhaps surprisingly so considering their basis on as-built records rather than final plans. However, the precast piles at Route U are relatively short; most of the pile length estimates were only about 4 ft less than the exhumed lengths. The error could be a result of differences in survey datum between the 1960s system and the system used for this project, the effect of using the average pile length (since only the total length of piling was reported), misinterpretation of the as-built records, or a combination of these explanations.

For the CIP piles at the Route WW site, pile driving records were available. Driving records generally provide more accurate information on the length of the individual piles than final plan documents. Comparisons between the actual exhumed lengths and the predicted lengths based on the driving records were generally within a few percent, as shown in Table 10. The difference in error values between the two sites suggests pile driving records provide more accurate pile length estimates than as-built plans.

Table 9: Route U precast pile length prediction from historical records.

Pile Number	Pile Top Elevation in Plans	Exhumed Pile Top Cutoff Elevation (ft)	Exhumed Pile Length (ft)	Estimated Lengths from Plans	% Error
1	295.44	292.51	23.50	19.94	-15.2
2	295.44	294.02	25.08	21.45	-14.5
4	295.44	292.43	23.50	19.86	-15.5
5	294.94	293.64	30.13	21.26	-29.4
6	294.94	293.69	30.17	21.62	-28.3
LTP	295.44	290.22	21.33	17.65	-17.3

Table 10: Route WW CIP pile length prediction from historical records.

Pile Number	Pile Top Cutoff Elevation in Plans (ft)	Exhumed Pile Top Cutoff Elevation (ft)	In Place Lengths from Driving records	Exhumed Pile Length (ft)	Predicted Exhumed Length Based on Driving Records (ft)	% Error
1	294.83	294.07	55	55.23	54.24	-1.8
2	294.83	290.07	55	50.90	50.24	-1.3
3	294.83	294.34	55	55.20	54.51	-1.3
4	294.83	293.41	55	55.19	53.58	-2.9
5	295.33	294.41	64	64.52	63.08	-2.2
8	295.33	294.45	62	62.40	61.12	-2.1

4.1.2   Parallel Seismic from SCPT measurements

A summary of the predicted pile tip depths (relative to the road elevation) from Parallel Seismic (PS) measurements performed with the SCPT at Route U (precast piles) is presented in Table 11. The actual pile tip depths were calculated from the exhumed pile length, pile cutoff elevation, and road elevation. Battering of piles was also taken into account. Time records and wave arrival picks can be found in Appendix E, and plots of wave arrivals versus time can be found in Appendix F. With the exception of Pile 1, the results from PS testing at Route U showed good agreement between the actual and predicted pile tip depths, with errors of generally less than about 8%. The reason for the poor results at Pile 1 is likely due to poor data collection procedures used on this first pile. A horizontal impact on the side of the bridge bent was erroneously used which did not produce reasonable results. All other data collection used a vertical impact directly above the pile of interest. For Piles 1 through 4, both the p-p and p-s methods provided similar results. For the battered piles (Pile 5 and Pile 8) the p-p wave arrivals were difficult to detect and no interpretation could be performed. The p-s data from the battered piles produced a negative slope for energy radiating from the pile due to the non-parallel condition between the SCPT and the battered pile. In both cases a clear change to a positive slope was observed which yielded a reasonable estimate of pile depth. It was surprising that the p-s data collected for Pile 5 with a long offset distance of 15.6 ft provided a reasonable estimate of the pile depth. It should also be noted that in all other cases the PS method underestimated the pile length.

Table 11: Route U precast pile tip depth predicted from Parallel Seismic testing using SCPT receiver.

Pile Number	SCPT	Actual Pile Tip Depth (ft)*	Predicted Tip Depth from p-p waves (ft) *	Predicted Depth from p-s waves (ft) *	Distance from SCPT to Pile (ft)	% Error p-p wave	% Error p-s wave
1	H-16-71	29.09	25[b]	24.1	6.3	-14%	-17.2%
2	H-16-71	29.16	26.7[a]	29.1[a]	5.0	-8.5%	-0.21%
3	H-16-72	Not exhumed	27.7[a]	28.0[a]	4.0	-	-
4	H-16-72	29.17	27.9[a]	27[a]	5.3	-4.4%	-7.5%
5**	H-16-73	34.18	ND	36.5[b]	15.6	-	6.8%
8**	H-16-74	Not exhumed	ND	32.2[b]	8.8	-	-

*relative to the elevation of the road surface (298.1)
ND – could not be determined from the data

[a] determined from model fitting
[b] determined from depth where slope changes
** Battered pile

A summary of the results from Parallel Seismic using the SCPT at Route WW (CIP piles) is presented in Table 12. Reasonable estimates of pile depth were obtained from measurements using p-s arrivals for Piles 1 and 2, with errors of 3.3% and 10.7%, respectively. Good quality p-s data was also obtained for Piles 3 and 4, however, due to a lack of penetration of the H-16-75 sounding it was not possible to identify the depth where a change in slope occurred. However, it was possible to infer that Pile 3 was at least 60 ft below the ground surface and Pile 4 was at least 55 ft below the ground surface. The p-s results from Pile 5, which is battered, showed a slope change at 50 ft which corresponds to a depth below the ground surface of about 68 ft. The p-s arrivals from Pile 8, which is also battered, did not show a definitive slope change and could not be interpreted. This was primarily due to insufficient penetration of SCPT sounding H-16-77.

 Unlike the results from Route U, the p-p arrivals could not be interpreted for any cases at Route WW. In most cases, p-p wave arrivals could only be identified at very shallow depths.

Table 12: Route WW CIP pile tip depth predicted from Parallel Seismic testing using SCPT receiver.

Pile Number	SCPT	Actual Pile Tip Depth (ft)*	Predicted Tip Depth from p-p waves (ft)	Predicted Depth from p-s waves (ft)	Distance from SCPT to Pile (ft)	% Error p-p wave	% Error p-s wave
1**	H-16-76	57.98	ND	59.9 [b]	9.2	-	3.3%
2	H-16-76	59.33	ND	52.9 [b]	17.5	-	10.7%
3	H-16-75	59.36	ND	>60	16.6	-	-
4**	H-16-75	58.64	ND	>55	8.3	-	-
5**	H-16-78	67.71	ND	68	24.5	-	0.43%
8**	H-16-77	65.60	ND	ND	18.3	-	-

*relative to the elevation of the road surface (298.5)
ND – could not be determined from the data
[b] determined from depth where slope changes
** Battered pile

4.1.3   Parallel Seismic from Borehole Measurements

A summary of the results from Parallel Seismic testing using Borehole 1 at Route U is presented in Table 13. In this case measurements were performed on Piles 1 through 4 using the sensor in Borehole 1. Therefore, source-to-receiver distances from 4.8 to 17.8 ft were used. The results from the measurements performed at short offset distances (4.8 and 4.9 ft) provided reasonable estimates of the pile depth. The p-s results from Pile 3 and Pile 4 at offset distance of 11.4 and 17.8 ft, showed arrivals that were too early for the large offset distances, as discussed in more detail below.   The p-p data for Pile 4 produced a significant underprediction (28%) of the length.

Measurements were also performed using Borehole 2 at Route U for testing precast Piles 1 through 4. The results from these tests are shown in Table 14. The results again show good agreement for measurements performed using close spacing and significant errors for the longest spacing. As noted above, long spacing p-s data from Piles 1 and 2 showed wave arrivals that were too early for the distance traveled. For example, Figure 33 shows the arrival times of the shear wave detected at Borehole 2 from an impact above Pile 1 located 17.8 ft away. The arrival times follow an expected bilinear shape, with a change in slope occurring at a depth of approximately 30 ft. However, the arrival times of the shear wave

between 0.005 and 0.01 sec is far too early for a source located 17.8 ft away in soil with a shear wave velocity of about 700 fps. Although the impact occurred over Pile 1, the energy likely radiated through the concrete bent to one of the closer piles (Pile 3 or 4). It would be easy to misidentify the length of the pile in this case.

Table 13: Route U precast pile tip depths predicted from Parallel Seismic testing using Borehole 1.

Pile Number	Actual Pile Tip Depth (ft)*	Predicted Depth from p-p waves (ft)*	Predicted Depth from p-s waves (ft)*	Distance from SCPT to Pile (ft)	% Error p-p wave	% Error p-s wave
1	29.09	30.8 [a]	33.7 [a]	4.8	5.8%	15.8%
2	29.16	27.9 [a]	29.3 [a]	4.9	-4.5%	0.3%
3	Not exhumed	28.2 [a]	ND	11.4	-	-
4	29.17	21.7 [a]	ND	17.8	-28%	-

*relative to the elevation of the road surface (298.1)
ND – could not be determined from the data
[a] determined from model fitting

Table 14: Route U precast pile tip depths predicted from Parallel Seismic testing using Borehole 2.

Pile Number	Actual Pile Tip Depth (ft)*	Predicted Depth from p-p waves (ft)	Predicted Depth from p-s waves (ft)	Distance from SCPT to Pile (ft)	% Error p-p wave	% Error p-s wave
1	29.1	19.9[a]	ND	17.8	-31.6%	-
2	29.2	27.9[a]	ND	10.7	-4.4%	-
3	Not exhumed	26.8[a]	26.1[a]	4.1	-	-
4	29.2	32.2[a]	27.7[a]	4.1	10.2%	-5.1%

*relative to the elevation of the road surface (298.1)
ND – could not be determined from the data
[a] determined from model fitting
*Determined using length of exhumed piles and known battering of the pile
** Battered pile
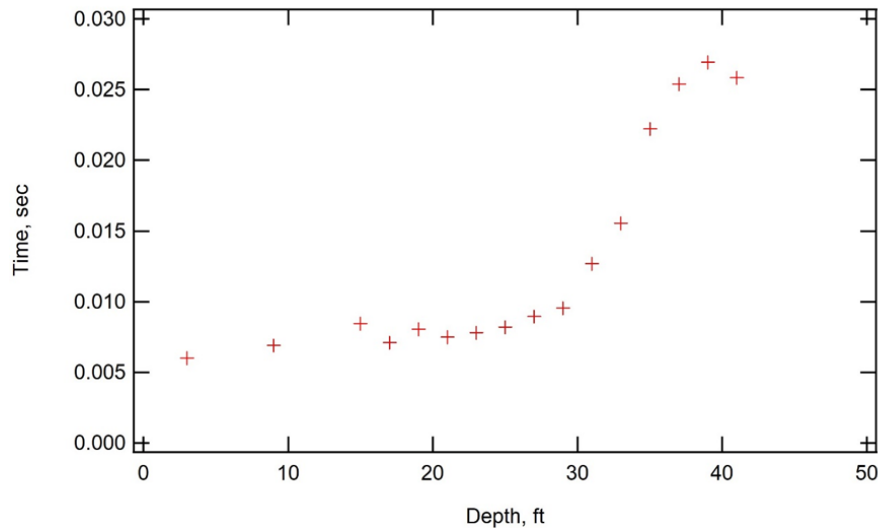
Figure 33: Wave arrivals at Borehole 2 from hitting above precast Pile 1 at Route U site.

The results from borehole measurements at Route WW are presented in Table 15 and Table 16. The results from Route WW were not successful, in part because the borehole did not extend deep enough to definitively detect a change in slope of wave arrivals. Generally speaking, good quality p-s data were collected for cases where the borehole was close to the pile (less than 5 ft). However, the borehole did not extend deep enough to detect a change in slope of the wave arrivals. It was possible to infer from measurements in Borehole 1 that Pile1 and Pile 2 were at least 60 ft long. All other pile measurements from Borehole 1 were over longer distances (14 to 35 ft) where the same problem of erroneously early arrivals was observed. Therefore, it was not possible to detect the pile lengths of Piles 3, 4, 5 and 8 from Borehole 1. As was the case with the SCPT at Route WW, it was not possible to interpret the p-p wave arrivals. In some cases, p-p arrivals could not be detected while in other cases p-p waves were detected but it was not possible to observe any change in slope of the wave arrivals. Therefore, detection of pile length from p-p measurements from Borehole1 was unsuccessful.

Table 15: Route WW CIP pile tip depths predicted from Parallel Seismic testing using Borehole 1.

Pile Number	Actual Pile Tip Depth (ft)*	Predicted Depth from p-p waves (ft)	Predicted Depth from p-s waves (ft)	Distance from SCPT to Pile (ft)	% Error p-p wave	% Error p-s wave
1	58.0	ND	>60 ft	4.8	-	-
2	59.3	ND	> 60 ft	4.1	-	-
3	59.4	ND	ND	13.8	-	-
4	58.6	ND	ND	22.9	-	-
5**	67.7	ND	ND	34.9	-	-
8**	65.6	ND	ND	34.9	-	-

*relative to the elevation of the road surface (298.5)
ND – could not be determined from the data
** Battered pile

Results from Borehole 2 at Route WW were consistent with what was observed at Borehole 1. For close spacings (<5 ft) between the piles and the boreholes, good quality p-s data were collected. Due to a lack of penetration depth it was not possible to definitively determine the depth where a change in slope occurred. However, based on the measured data it could be inferred that Pile 3 was at least 60 ft deep and Pile 4 was about 60 ft deep. The p-s data collected from piles at greater distances (in this case Pile 1 and Pile 2) showed arrival times that were far too early for the wave propagation distances. Therefore, the depths of Piles 1 and 2 could not be determined from Borehole 2.

Table 16: Route WW CIP pile tip depths predicted from Parallel Seismic testing using Borehole 2.

| Pile Number	Actual Pile Tip Depth (ft)*	Predicted Depth from p-p waves (ft)	Predicted Depth from p-s waves (ft)	Distance from SCPT to Pile (ft)	% Error p-p wave	% Error p-s wave
1	58.0	ND	ND	22.6	-	-
2	59.3	ND	ND	13.8	-	-
3	59.4	ND	>60	5.1	-	-
4	58.6	ND	60 [b]	5.3	-	2.4%
5**	67.7	Not tested	Not tested	Not tested	-	-
8**	65.6	Not tested	Not tested	Not tested	-	-

*relative to the elevation of the road surface (298.5)
ND – could not be determined from the data
[b] determined from depth where slope changes
** Battered pile

4.1.4   SE-IR on Cut Piles

Pile lengths determined from SE measurements on the cut piles at the Route U site are presented in Table 17. The predicted lengths from the SE measurements were calculated from the two-way travel time and the compression wave velocity of the pile using Eq. 1. The predicted length from the IR method was determined from the frequency span between peaks and the compression wave velocity using Eq. 2. All SE and IR records from each site can be found in Appendix G. In practice, the compression wave velocity used in Eq. 1 and 2 must be either assumed or measured in the exposed portion of the pile. Table 18 presents the range of compression wave velocities measured in the exhumed piles from Route U over different measurement intervals as well as the velocity measured in Pile 6 on the exposed section prior to exhumation. The results show that under the best measurement condition (instrumenting over long lengths of the exhumed piles) the measured velocities on a single pile varied by 2% to 5%. The velocity measured on the exposed portions of Pile 6 is in good agreement with the full length measurements on the exhumed pile (within 1%). The length estimates presented in Table 17 used the average (longest-span) velocities measured on the exhumed piles.

Although the quality of data was very good and the compression wave velocities were accurately measured for the piles at Route U, in all cases the length of the piles was underestimated by the SE and IR methods. The length was underpredicted by about 3 to 5 ft (10 to 20 percent) in all cases, which suggests the reflected waves detected with the SE and IR methods are primarily from the change in area occurring at the start of the tapered section of the pile. It was not possible to identify a second reflection from the tip of the Route U precast piles.

The data analysis from testing of the CIP piles at Route WW is presented in Table 17. Compression wave measurement on the exhumed piles is presented in Table 18. For the CIP piles, the errors in predicted

length were typically less than about 6%. With the exception of Pile 2, the length was underpredicted from the SE-IR measurements.

As shown in Table 21, the measured velocity values from each site were remarkably consistent, with coefficient of variation value of 5.3% and 3.2% for the precast piles and CIP piles, respectively.

Table 17: Route U precast pile length from Sonic Echo and Impulse Response after bridge removal.

Pile Number	Measured Length of Exhumed Pile (ft)	Predicted Length from SE (ft)	Predicted Length from IR (ft)	Wave velocity Used (fps)*	% Error SE	% Error IR
1	23.5	19.1	20.5	11,350	-18.7%	-12.8%
2	25.1	22.6	22.4	12,725	-9.9%	-10.8%
3	Not exhumed	20.0	20.1	11,620	-	-
4	23.5	19.5	20.1	11,166	-17.0%	-14.4%
5	30.1	26.5	29.3	11,544	-11.9%	-2.7%
6	30.2	25.5	24.8	11,310	-15.6%	-17.9%
7	Not exhumed	25.3	25.7	11,620	-	-
8	Not exhumed	23.8	24.7	11,620	-	-
LTP	21.33	18.3	-	11,620	-14.2%	-

Table 18: Compression wave velocity measurements from exhumed precast piles at Route U.

Pile Number	Velocity of Lower half (fps)	Velocity of Upper half (fps)	Average Velocity (fps)*
1	12,947	10,240	11,350
2	13,152	12,288	12,725
3	Not exhumed	Not exhumed	Not exhumed
4	10,803	11,538	11,166
5	10,889	12,288	11,544
6	11,095	11,538	11,310
7	Not exhumed	Not exhumed	Not exhumed
8	Not exhumed	Not exhumed	Not exhumed
LTP	10,231	11,494	10,845
6-field**	N/A	N/A	11,837

*calculated from the travel times over the upper and lower of the pile
** velocity of Pile 6 measured on exposed section in the field prior to exhumation

Table 19: Route WW CIP pile length from Sonic Echo and Impulse Response after bridge removal.

Pile Number	Measured Length of Exhumed Pile (ft)	Predicted Length from SE (ft)	Predicted Length from IR (ft)	Wave velocity Used (fps)*	% Error SE	% Error IR
1	55.2	53.4	50.7	13,100	-3.3%	-8.2%
2	50.9	52.8	51.7	13,889	3.8%	1.6%
3	55.2	51.9	48.2	13,100	-6.0%	-12.7%
4	55.2	51.5	53.3	14,150	-6.7%	-3.4%
5	64.5	61.0	62	13,797	-5.4%	-3.9%
6	Not exhumed	Not tested	Not tested	N/A	N/A	N/A
7	Not exhumed	Not tested	Not tested	N/A	N/A	N/A
8	62.4	58.5	58.8	13,797	-6.3%	-5.8%

Table 20: Compression wave velocity measurements from exhumed CIP piles at Route WW.

Pile Number	Interval Velocity from Lower Portion of Pile (fps)	Interval Velocity from Upper Portion of Pile (fps)	Velocity from Longest Interval (fps)
1	12,295	12,500	13,100
2	13,274	14,705	13,889
3	12,711	13,157	13,100
4	13,889	14,423	14,150
5	13,636	14,423	13,797
6	Not exhumed	Not exhumed	Not exhumed
7	Not exhumed	Not exhumed	Not exhumed
8	13,889	14,019	13,797
3-field*	N/A	N/A	13,227

* velocity of Pile 3 measured on exposed section in the field prior to exhumation

Table 21 Average and standard deviation of measured pile velocities at Route U and Route WW

Site	Average Velocity (fps)	Standard Deviation (fps)	Coefficient of Variation (%)
Route U	11,540	606	5.3
Route WW	13,580	428	3.2

4.1.5   SE Measurements on Piles Before Bridge Removal

Sonic-Echo measurements were performed on two of the piles at each bridge site prior to removal of the bridge superstructure, as described in Section 3.3.3. The objective of these measurements was to determine if the reflected return from the tip of the pile could be detected when the pile remained connected to the bridge superstructure. When the pile remains connected to the bridge superstructure the waves propagating in the pile are much more complicated and difficult to interpret. To aid in the interpretation, two receivers were used such that downward moving waves will arrive first on the upper receiver and upward propagating waves reflecting from the tip of the pile will arrive first on the lower geophone. Unfortunately, attempts to detect reflections from the tip of the pile while the pile remained connected were not successful at either site. Example results from precast Pile 7 at the Route U site are presented in Figure 34. No indication of a reflected wave arrival from the pile tip is evident in these records. For comparison, the results obtained from the same pile after the bridge superstructure was removed is shown in Figure 35. Similar results were obtained from testing CIP piles at the Route WW site.
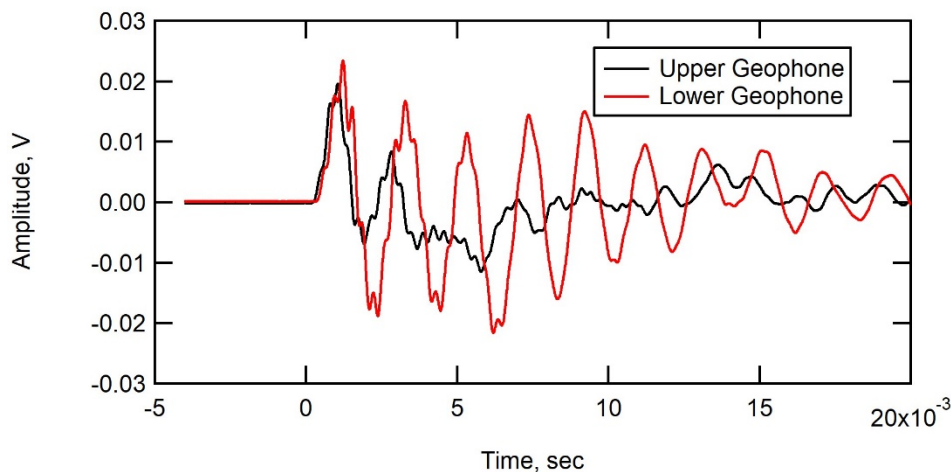
Figure 34: Time records from SE measurements performed on precast Pile 7 prior to Route U bridge removal.
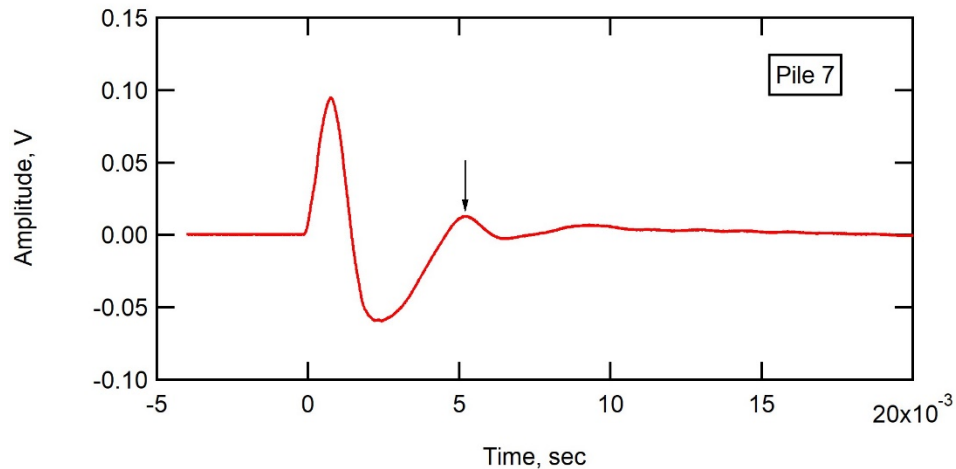
Figure 35: Time record from SE measurement performed on precast Pile 7 after Route U bridge removal.

4.2   Pile Condition

4.2.1   Condition Information from Geophysical Observations

Geophysical methods such as SE and IR can be used in some instances to obtain information about the condition of the pile. If large changes in cross-sectional area, velocity or density occur a reflection may be detected. No evidence of condition flaws was observed in any of the geophysical records. Subsequent inspection and testing of the exhumed piles also did not reveal any significant problems with the condition of the piles. Therefore, it was not possible to test the effectiveness of these methods for condition assessment from the results of this study.

4.2.2   Condition of Exhumed Piles

As described in Section 3.7, six precast and six CIP piles were exhumed after completing the static load tests and pile restrikes. Photographs of the exhumed precast piles from the Route U site are shown in Figure 36, Figure 37, and Figure 38. The photographs indicate the precast piles were in excellent condition, with no evidence of any significant concrete cracking or surface damage. The most noteworthy observation regarding the precast piles was the strong adhesion of sand to the tips of the piles. In fact, application of a high-pressure water jet to the tips of the pile was mostly incapable of removing the sand, which appeared to be chemically bonded to the pile concrete. The cemented sand increased the effective size of the precast piles, which could have increased the load capacity of the precast piles.

Figure 36: Exhumed precast piles.

Figure 37: Photographs of tips of exhumed precast piles.

Figure 38: Close-up view of tip of exhumed precast pile showing sand adhered to pile surface.

Photographs of the CIP piles exhumed from the Route WW site are shown in Figure 39. In general, the exhumed piles appeared to be in excellent condition, particularly considering their 50-year age. For each pile, there was an approximately 5-ft long section with visible surface corrosion. The corroded length of each pile was within the top 10 ft of the pile, which corresponds to the probable zone of groundwater fluctuation. The CIP pile bridge is approximately 1 mile from the Mississippi River, so the groundwater is relatively shallow, and the depth likely does not vary greatly. There was no evidence of surface corrosion along the exhumed CIP piles below depths of 10 ft.

Figure 40 is a photograph showing a close-up view of the corroded length of one exhumed CIP pile. To further examine the extent of corrosion, measurements of steel pipe thickness were made at 19 locations using calipers, with results shown in Table 22. The measurement locations included the top of each exhumed pile as well as 13 cross-sections exposed by cutting the piles. The cuts were made using a circular demolition saw. Approximately half of the cut locations had visible surface corrosion while the other half did not. Sample photographs of the cut cross-sections are shown in Figure 41, which includes one section with corrosion and one without. The photographs indicate no visible difference in the steel condition between the two locations. Caliper measurements of steel thickness (Table 22) also did not indicate any difference in thickness. In fact, the average steel thickness measured in sections without visible surface corrosion was 0.266 in., which is actually 2.5 percent less than the average steel thickness measured in sections with visible surface corrosion, 0.272 in. For both sets of cross-sections, steel thickness measurements were relatively uniform, with coefficients of variation less than 5 percent. Based on the 1960s standard for CIP piles, the minimum wall thickness for CIP piles was either 0.23 or 0.25 in. As shown in Appendix A, the value is unclear; regardless, the measured thickness values in locations with and without corrosion are greater than the specified values.

Figure 39: Photographs of exhumed CIP piles: (a) full length and (b) length of pile without surface corrosion in foreground and length of pile with surface corrosion in background. Note that although it is marked as Pile 6 this is Pile 8.

Figure 40: Close-up view of segment of exhumed CIP pile with surface corrosion. White line is location of future cut to expose pile cross-section.
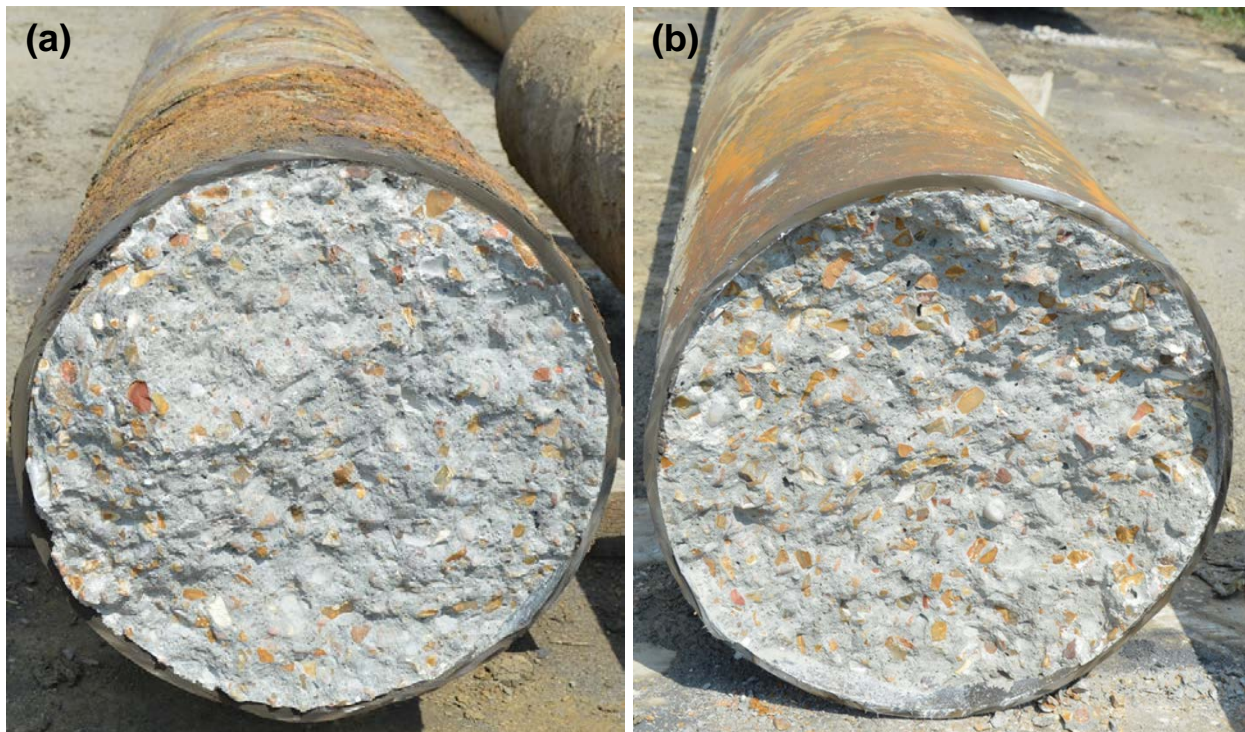
Figure 41: Cross sections of exhumed CIP piles after making cuts at select locations: (a) location with apparent surface corrosion and (b) location with negligible surface corrosion.

Table 22: Caliper-measured thickness of steel pipe of exhumed CIP piles at select cut locations.

Pile Number	Cut Location	Surface Corrosion?	Thickness Measurements, in.			Average Thickness, in.
1	Pile Top	No	0.264	0.260	0.270	0.265
	Top Cut	Yes	0.264	0.256	0.260	0.260
	Bottom Cut	No	0.264	0.262	0.260	0.262
2	Pile Top	No	0.275	0.258	0.238	0.257
	Top Cut	Yes	0.290	0.268	0.274	0.277
	Bottom Cut	No	0.255	0.268	0.283	0.269
3	Pile Top	No	0.250	0.262	0.270	0.261
	Top Cut	Yes	0.265	0.265	0.269	0.266
	Bottom Cut	No	0.255	0.265	0.258	0.259
4	Pile Top	No	0.287	0.265	0.275	0.275
	Top Cut	Yes	0.265	0.261	0.265	0.268
	Upper Middle Cut	Yes	0.255	0.275	0.300	0.278
	Lower Middle Cut	No	0.265	0.255	0.248	0.256
	Bottom Cut	No	0.264	0.260	0.270	0.265
5	Top Cut	Yes	0.275	0.295	0.270	0.280
	Bottom Cut	No	0.275	0.280	0.265	0.273
8	Pile Top	No	0.280	0.284	-	0.282
	Top Cut	Yes	0.283	0.285	0.280	0.283
	Bottom Cut	No	0.270	0.269	0.264	0.268

4.3 Load Capacity

Results from the static load tests and dynamic analysis of restrike data are presented in this section. All estimates of pile load capacity, including historical values and static predictions, are presented in a summary at the end of this section.

4.3.1 Static Load Test Results

Axial load-displacement curves for the top of test piles are shown in Figure 42. Load tests for the precast test pile and CIP test pile were both terminated upon failure of the existing capping beam used as the reaction frame for the test load. Both bridges used the same capping beam design, and for both sites, the ultimate test load was similar: 268 kips for the Route U precast pile load test, and 247 kips for the Route WW CIP pile load test. Failure of the capping beam at the Route U, precast pile bridge was relatively ductile, characterized by several cracks covering most of the height of the capping beam. The precast pile load test at Route U was also characterized by significant lifting of the existing bridge deck for the last three load increments, with displacements of approximately 0.25 in. for each increment. The test was terminated when the load could not be increased further as the ram of the hydraulic cylinder chased the upward displacement of the capping beam. Although failure of the reaction system was the reason for terminating the precast pile load test, the shape of the load-displacement curve of Figure 42 indicates the precast test pile was approaching its ultimate geotechnical resistance when the test was terminated at 268 kips.

For the CIP pile bridge, fracture of the capping beam was more sudden, producing an audible noise and a visible crack that appeared to extend the full depth and full width of the beam. Based on the load-displacement curve shown in Figure 42, the CIP test pile had not yet achieved ultimate geotechnical resistance at the maximum test load of 247 kips. One potential explanation of the greater beam capacity at the precast bridge is that the greater displacement of the reaction piles, which are shorter at the precast bridge, resulted in wider load distribution along the precast capping beam and therefore a more ductile response.
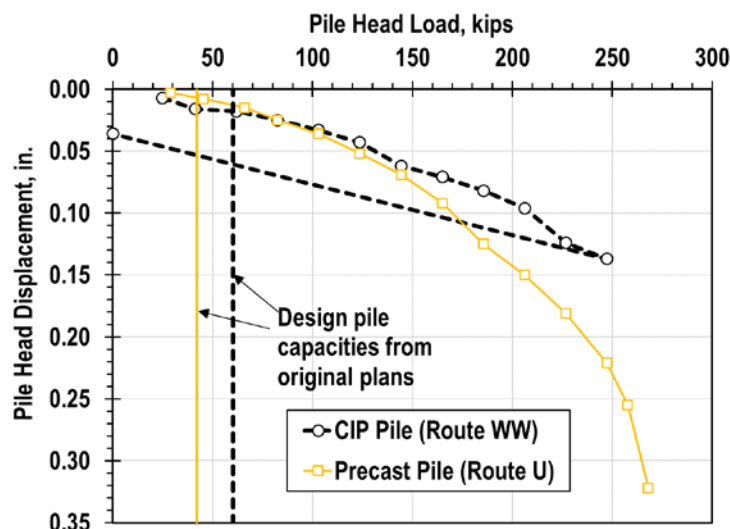
Figure 42: Load-displacement curves for the top of test piles.

4.3.2   Dynamic Analysis of Restrike Tests

Results of the dynamic pile load tests are presented in the GRL Engineers, Inc. reports of Appendix D and summarized in Table 23. The restrike result for the static load test piles are shown in bold text in Table 23. The reports note that for test piles at both bridges, a larger hammer would be necessary to fully mobilize end bearing, so the end bearing and therefore total capacity values listed in Table 23 are lower bound values. In addition, the report for the precast pile tests at the Route U site notes dynamic analysis of tapered piles is complicated, so there is perhaps greater uncertainty in the results for the precast piles.

Table 23: Results of dynamic analysis of pile restrike tests. Row with bold text is the static load test pile for the precast bridge.

Site (Pile Type)	Bent	Pile	Measured Length, ft	Pile Inclination	Capacity, kips		
					Side Resistance	End Bearing	Total
Route U (Precast)	**East End**	**North Interior**	**21.3**	**Vertical**	**187**	**60**	**247**
	West Middle	North Exterior	30.1	Vertical	265	70	335
	West Middle	North Interior	30.2	Vertical	236	65	301
	West End	North Exterior	23.5	Battered	181	65	246
	West End	South Interior	25.1	Vertical	144	62	206
Route WW (CIP)	West End	North Exterior	55.2	Battered	250	18	268
	West End	**North Interior**	**50.9**	**Vertical**	**221**	**80**	**301**
	West End	South Interior	55.2	Vertical	223	78	301
	West End	South Exterior	55.2	Battered	228	40	268
	West Middle	North Exterior	60.2	Battered	221	22	243
	West Middle	South Exterior	62.4	Battered	195	34	229

4.3.3   Summary of Load Capacity Estimates

Estimates of load capacity from the historical plans, available pile driving records, static analyses, static load tests, and dynamic analyses of restrikes are summarized in Table 24 for both pile types. For each pile type, one column lists the actual value of predicted capacity in kips and the adjacent column lists the value as a percentage of the maximum load measured during the static load test. Since the static load tests were terminated upon failure of the reaction beam, the maximum applied load represents a lower bound on the geotechnical resistance of the test pile, although as explained in Section 4.3.1, the shape of the load-displacement curve for the test precast pile at Route U suggests the ultimate load was likely close to the ultimate resistance of the test pile.

Table 24: Summary of geotechnical axial load capacity of piles in compression from various prediction and test methods.

Method	Route U (Precast Piles)		Route WW (CIP Piles)	
	Predicted Capacity, kips	Percent of Max Load from Static Load Test	Predicted Capacity, kips	Percent of Max Load from Static Load Test
Value from historical plans	28 or 42	10 or 16	60	24
Values from pile driving record (dynamic formulas):	N/A			
Range (all piles)			60 to 115	24 to 47
Test pile			67 or 83	27 or 34
Static predictions (University):				
Eslami and Fellenius (CPT)	280	104	230	93
Meyerhoff (SPT)	N/A		213	86
Brown (SPT)	130	49	346	140
Alpha / Nordlund	574	214	334	111
Static prediction (MoDOT):				
LCPC (CPT)	110	41	335	136
Alpha / Nordlund	106	40	480	194
Static load test	**>268**	**100**	**>247**	**100**
Dynamic analysis of restrike on Load Test Pile	247	92	301	122

For both pile types, the load capacity values from the historical plans are significantly less than the maximum applied loads from the static load tests – at most 24 percent of the applied loads. This finding suggests that, as suspected, the values listed on the historical documents are allowable values based on a conservative factor of safety. The results of the load test indicate the working factor of safety was at least four. For the CIP bridge, the capacity values listed on the historical pile driving record document were also significantly lower than the maximum applied test load, which is unsurprising since dynamic pile driving formulas typically include a conservative factor of safety to account for the uncertainty associated with the methods.

As discussed in Section 3.5, the static prediction methods produce significantly variable estimates of capacity, reflecting the inherent uncertainty of predicting driven pile capacity. As discussed above regarding Figure 42, the load-displacement results for the precast pile suggest the test pile was approaching ultimate geotechnical resistance at the maximum applied load of 268 kips. The maximum applied test load is at least two times greater than all of the static predictions, except for the prediction based on the alpha and Nordlund methods. The alpha and Nordlund method prediction was the only static prediction to consider the taper of the precast piles. For the CIP pile, the maximum load applied during the static load test was slightly greater than the value predicted by the Meyerhoff SPT method, which was the lower bound of the static predictions. The other static predictions for the CIP pile were similar to or slightly greater than the maximum applied load.

The dynamic analysis of restrike data (via CAPWAP) predicted capacity values that are relatively close to the maximum applied load from the static load tests. The restrike analysis results therefore lend support to the idea that the test piles were approaching ultimate geotechnical resistance when the reaction beams failed. However, the dynamic analysis reports noted that the interpreted end resistance values were likely underestimated because the pile driving hammer from the restrike was not too light to transfer sufficient load to the pile tip. Thus, although both the static and dynamic field measurements yielded predictions that are less than the true ultimate geotechnical resistance, the results were sufficiently close to ultimate to confirm that (1) capacity values from historical documents were conservative by a factor of at least four and (2) static prediction methods were highly variable but preferable to the historical document values, particularly if an appropriate static prediction method is applied.

5. Conclusions

The national survey of transportation agencies from NCHRP Synthesis 505 revealed that existing foundations are commonly reused to reduce project costs, accelerate construction schedules, and satisfy environmental and various other project constraints. The same survey also revealed that practices for reusing foundations, and in particular practices for investigating existing foundations, vary widely, with little established guidance. This research project was performed to examine the efficacy of various investigation techniques for evaluating existing pile length, condition, and load capacity, and to evaluate the condition and load capacity of two specific types of driven piles after 50 years of service.

5.1 Summary of Significant Findings

The following conclusions and observations can be drawn from the investigations performed in this study:

- Pile length estimates from pile driving records for CIP piles at Route WW were within 2 or 3 percent of the exhumed pile lengths. Pile length estimates from as-built plans for the precast piles at Route U were 15 to 30 percent shorter than exhumed pile lengths. These findings suggest the specific length information contained in pile driving records is more accurate than as-built markups of final plans, which often report total length of piling rather than specific information.

- The use of MoDOT's SCPT rig for Parallel Seismic (PS) testing of unknown foundation conditions appears to be viable. The lack of a vertically oriented sensor did not appear to be a significant detriment to PS data interpretation. The primary limitation may be the inability to penetrate stiffer materials that the pile may be founded on, as was the case at the Route WW site.

- Parallel seismic measurements from both the SCPT and borehole configurations produced reasonable results (generally within 8% or less) when the sensor was positioned close to the pile of interest (5 ft or less). At large distances between the pile and the sensor (10 to 35 ft in this study) there was a greater possibility for misinterpretation of the data. Of particular note was the observation that at large distances it is possible to record first arrivals from a closer pile than the one over which the energy was excited. The response may look reasonable apart from recognition that the energy is arriving far too early.

- Both the p-p and p-s approach to interpreting PS data can yield reasonable results. However, in this study the p-s arrivals were more easily identified and interpreted than the p-p arrivals, especially for the CIP piles at the Route WW site.

- Testing battered piles violates the "parallel" assumption in the PS method. Therefore, the arrival time versus depth relationship is more complex. Approximate depths can still be identified by a change in slope of the wave arrival plot when the pile is battered toward the sensor borehole.

- The quality of data from the SE/IR measurements performed on the cut piles at the Route U and Route WW sites was very good and easily interpreted. However, results from the Route U site produced a significant underestimation of the length (by as much as 20% in some cases). The underestimation was consistently in the range of about 3 to 5 ft. This suggests that the reflection originated from the change in area over the tapered section of the pile. Reflections from the tip of the pile were not evident. Therefore, caution should be used when estimating depths of tapered piles with the SE/IR method. Length estimates at the Route WW site with the non-tapered CIP piles were generally within about 6% and were typically underestimated by the SE/IR results.

- SE measurements on piles at the Route U and Route WW sites prior to removal of the bridge superstructure were not successful in identifying a reflected arrival from the pile tip. A combination of the high attenuation of the reflected wave and the complex vibrations within the pile and connected superstructure did not allow for effective detection.

- Compression wave velocities measured on exposed pile sections in the field were consistent with values measured on the exhumed piles. Therefore, in practice wave velocities used in the SE/IR interpretation can be obtained by performing interval velocity measurements on exposed sections of the pile. In addition, variability in the velocities measured on different piles at the same site was generally low with COV values in the range of 3 to 5 %,

- All twelve exhumed piles (six of each pile type) appeared to be in excellent condition.

    o For CIP piles, there was visible surface corrosion on the outside of the steel pipe piles, but caliper measurements of the steel thickness did not indicate any significant difference in steel thickness between cuts made within the corroded lengths and cuts made in zones of the pile with no evident corrosion. The average thickness measurement in the corroded sections and in sections without corrosion was greater than the specified steel thickness from the 1960s standard specifications. The visible surface corrosion was only evident along an approximately 5-ft long section of each pile that corresponded to the depth of groundwater fluctuation.

    o For precast piles, there was no evidence of deterioration. Sand was adhered along the bottom approximately 5 ft of each of the exhumed precast piles, increasing the effective diameter of the tapered pile tips. The sand appeared to be chemically bonded to the pile concrete; a high-pressure water jet was mostly incapable of removing the sand.

- Estimates of the axial load capacity of the existing foundations varied widely:

    o Values listed on historical documents were the least, and static load test results indicate the historical values are quite conservative: the precast test pile was loaded to seven times the historical design capacity, and the CIP test pile was loaded to four times the historical design capacity. Both tests were terminated upon failure of the capping beam, so the maximum test loads do not necessarily represent ultimate geotechnical resistance, although the load-displacement curve for the precast pile indicated the pile was likely approaching an ultimate condition.

    o Dynamic analysis of restrike data yielded estimates of axial capacity similar to the maximum loads applied during the static load tests. The dynamic values can also be considered lower bound estimates of capacity because the pile driving hammer used to restrike the piles had insufficient energy to transfer significant loads to the pile tips.

    o Static methods of predicting driven pile capacity produced a wide range of estimates. Some of the static prediction methods produced estimates that were less than the maximum load applied during static load testing while estimates from other methods were greater than the applied load; however, all of the static method estimates were greater than the values listed on the historical plan documents.

5.2   Recommendations

A number of recommendations regarding investigation and analysis of existing foundations being considered for reuse based on the results of this research:

- Parallel seismic measurements to estimate length should be performed at distances of 5 ft or less if possible. At longer distances, travel times should be checked to be sure energy is not radiating from closer piles. Vertical impacts should be used to excite energy in the piles.

- Parallel seismic measurements of battered piles should be performed such that the batter direction is either towards the borehole (or SCPT) or the plane of batter is perpendicular to the borehole (or SCPT). Measurements with the pile battered away from the sensor may overestimate the length.

- The length of taper of a tapered pile may need to be added to the length determined from SE-IR measurements if only a single reflection is evident in the response.

- Velocity values for use in SE and IR measurements should be obtained from direct velocity measurements on exposed portions of the foundations. Use of assumed values of velocity may produce erroneous length estimates.

- Absent field methods for estimating pile length, pile driving records likely provide the most accurate pile length information. The pile driving records are also frequently more clear than final plans or as-built plans, which may report only total length of piling. Pile driving records are also less readily located than final plans or even as-built plans, as the experience of this project suggests. The findings of this study suggest the extra legwork required to locate the pile driving records is worthwhile if the records are located.

- Condition assessment is a challenging component of foundation reuse investigations. However, as observed for this research and documented elsewhere (e.g. Boeckmann and Loehr, 2017), most ground conditions provide good protection to deterioration compared to above-ground conditions. Steel piles do typically experience some corrosion in the zone of groundwater fluctuation, but severe corrosion typically only occurs in the presence of aggressive groundwater (e.g. at contaminated sites). Test pits and sampling of foundations via concrete coring and steel coupons can provide useful reassurance, particularly if the test pits can expose the area of groundwater fluctuation.

- Axial load capacity of existing piles being considered for reuse should not be designed based on values listed in historical documents. New values of load capacity should be estimated from static prediction methods, preferably based on new subsurface investigation information, or from static or dynamic load tests.

- Static load tests using the existing bridge as a reaction frame are feasible, as shown in the tests for this project and for the Maine DOT Haynesville Bridge project. The feasibility of such tests is likely greater if the tests are proof tests based on design loads, rather than tests to ultimate resistance. For the Haynesville Bridge project, the test piles were re-connected and reused.

- Dynamic load tests from restrikes of existing piles are also a useful method for estimating load capacity of existing driven piles, particularly for projects where a pile driving hammer is to be mobilized for installation of additional driven piles.

References

Akkus, H. (2018), *Calculated versus Measured Static Capacity for Two Pile Types*, Thesis Presented to the University of Missouri, Anticipated May 2018.

Boeckmann, A. and J.E. Loehr (2017), *NCHRP Synthesis Report 505 – Current Practices and Guidelines for the Reuse of Bridge Foundations*, Transportation Research Board.

Browne, T.M., T.J. Collins, M.J. Garlich, J.E. O'Leary, D.G. Stromberg, and K.C. Heringhaus (2010), *Underwater Bridge Inspection*, Report No. FHWA-NHI-10-027, Federal Highway Administration, Washington, D.C.

Butcher, A.P., J.J.M. Powell, and H.D. Skinner (2006), *Reuse of Foundations for Urban Sites: A Best Practice Handbook*, IHS BRE Press, Hertfordshire, United Kingdom.

Jalinoos, F. (2015), "Reusing Bridge Foundations," *Public Roads*, FHWA-HRT-16-001, Vol. 79, No. 3, November/December 2015 [Online]. Available: http://www.fhwa.dot.gov/publications/publicroads/15novdec/05.cfm

Jalinoos, F., M.A. Mulla, and V.R. Schaefer (2016), "Foundation Reuse and Enhancement," *GEOSTRATA*, May/June 2016, pp. 52-57.

Johnson, A.P. and M.R. Chauvin (2013), "Evaluating Timber Piles," *Civil and Structural Engineer News*, February 2013 [Online]. Available: http://cenews.com/article/9175/evaluating-timber-piles

Wightman, W. E., F. Jalinoos, P. Sirles, and K. Hanna, *Application of Geophysical Methods to HighwayRelated Problems,* Publication FHWA-IF-04-021, Federal Highway Administration, Washington, D.C., 2004

Appendix A – Existing Bridge Documentation

Detailed description of contents is included in Section 3.2.

Driven Pile excerpt from 1961 MoDOT Standard Specifications (7 sheets, 2 pages/sheet)
Final plans for existing bridge A2141 (CIP piles) (4 sheets)
As-built ("Finished") plan sheet for existing bridge A2141 (CIP piles) (1 sheet)
MoDOT standards sheet for CIP piles from 1962 (1 sheet)
Record of pile driving for CIP piles (1 page)
Historical boring logs for existing bridge A2141 (CIP piles) (7 pages)
MoDOT geotechnical report for replacement of existing CIP pile bridge (41 pages)
Final plan sheet for existing bridge N0771 (Precast piles) (1 sheet)
As-built ("Finished") plans for existing bridge N0771 (Precast piles) (4 sheets)
MoDOT standards sheet for precast piles from 1962 (1 sheet)
MoDOT geotechnical report for replacement of existing precast pile bridge (14 pages)

To view appendices, see separate file at:

https://library.modot.mo.gov/RDT/reports/TR201714/cmr18-008_app.pdf

Appendix B – CPT Soundings and Downhole Boring Logs

To view appendices, see separate file at:

https://library.modot.mo.gov/RDT/reports/TR201714/cmr18-008_app.pdf

Appendix C – Pile Capacity Calculations

Discussion of contents is included in Section 3.5.

To view appendices, see separate file at:

https://library.modot.mo.gov/RDT/reports/TR201714/cmr18-008_app.pdf

Appendix D – Reports from Dynamic Analysis of Restrike Tests

Discussion of contents is included in Sections 3.6 and 4.3.

To view appendices, see separate file at:

https://library.modot.mo.gov/RDT/reports/TR201714/cmr18-008_app.pdf

Appendix E – Parallel Seismic Time Records

To view appendices, see separate file at:

https://library.modot.mo.gov/RDT/reports/TR201714/cmr18-008_app.pdf

Appendix F – Parallel Seismic Wave Arrival

To view appendices, see separate file at:

https://library.modot.mo.gov/RDT/reports/TR201714/cmr18-008_app.pdf

Appendix G – Sonic Echo / Impulse Response Data

To view appendices, see separate file at:

https://library.modot.mo.gov/RDT/reports/TR201714/cmr18-008_app.pdf